Architected Origami Materials: How Folding Creates Sophisticated Mechanical Properties

Suyi Li,* Hongbin Fang,* Sahand Sadeghi, Priyanka Bhovad, and Kon-Well Wang*

Origami, the ancient Japanese art of paper folding, is not only an inspiring technique to create sophisticated shapes, but also a surprisingly powerful method to induce nonlinear mechanical properties. Over the last decade, advances in crease design, mechanics modeling, and scalable fabrication have fostered the rapid emergence of architected origami materials. These materials typically consist of folded origami sheets or modules with intricate 3D geometries, and feature many unique and desirable material properties like auxetics, tunable nonlinear stiffness, multistability, and impact absorption. Rich designs in origami offer great freedom to design the performance of such origami materials, and folding offers a unique opportunity to efficiently fabricate these materials at vastly different sizes. Here, recent studies on the different aspects of origami materials—geometric design, mechanics analysis, achieved properties, and fabrication techniques—are highlighted and the challenges ahead discussed. The synergies between these different aspects will continue to mature and flourish this promising field.

1. Introduction

Origami is a craftsman art of folding paper into decorative shapes. It first appeared in East Asia over four centuries ago[1] and has since become a popular subject among educators,[2–5] mathematicians,[6,7] architects,[8] physicists,[9] and engineers.[10–12] Especially, the seemingly infinite possibilities of folding flat sheets into sophisticated 3D shapes have inspired a wide variety foldable structures of vastly different sizes: from large-scale deployable spacecraft[13,14] and kinetic buildings,[15–17] to mesoscale self-folding robots[18–25] and biomedical

devices,[26,27] to small-scale nano-[28–30] and DNA origamis.[31] A common theme in these studies is to exploit the sophisticated shape transformations from folding. For example, an origami robot is typically fabricated in a 2D flat configuration and then folded into the prescribed 3D shape to perform its tasks. The origamis have been treated essentially as linkage mechanisms in which rigid facets rotate around hinge-like creases (aka "rigid-folding origami"). Elastic deformation of the constituent sheet materials or the dynamics of folding are often neglected. Such a limitation in scope indeed resonates the origin of this field, that is, folding was initially considered as a topic in geometry and kinematics.

However, the increasingly diverse applications of origami require us to understand the force-deformation relationship and other mechanical properties of folded structures. Over the last decade, studies in this field started to expand beyond design and kinematics and into the domain of mechanics and dynamics. Catalyzed by this development, a family of *architected origami materials* quickly emerged (**Figure 1**). These materials are essentially assemblies of origami sheets or modules with carefully designed crease patterns. The kinematics of folding still plays an important role in creating certain properties of these origami materials. For example, rigid folding of the classical Miura-ori sheet induces an in-plane deformation pattern with auxetic properties (aka negative Poisson's ratios).[32,33] However, elastic energy in the deformed facets and creases, combined with their intricate spatial distributions, impart the origami materials with a rich list of desirable and even unorthodox properties that were never examined in origami before. For example, the Ron-Resch fold creates a unique tri-fold structure where pairs of triangular facets are oriented vertically to the overall origami sheet and pressed against each other. Such an arrangement can effectively resist buckling and create very high compressive load bearing capacity.[34] Other achieved properties include shape-reconfiguration, tunable nonlinear stiffness and dynamic characteristics, multistability, and impact absorption.

Since the architected origami materials obtain their unique properties from the 3D geometries of the constituent sheets or modules, they can be considered a subset of architected cellular solids or mechanical metamaterials.[35–39] However, the origami materials have many unique characteristics. The rich geometries of origami offer us great freedom to tailor targeted

Prof. S. Li, S. Sadeghi, P. Bhovad
Department of Mechanical Engineering
Clemson University
Clemson, SC 29631, USA
E-mail: suyil@clemson.edu

Prof. H. Fang
Institute of AI and Robotics
Fudan University
Shanghai 200433, China
E-mail: fanghongbin@fudan.edu.cn

Prof. H. Fang, Prof. K.-W. Wang
Department of Mechanical Engineering
University of Michigan
Ann Arbor, MI 48109, USA
E-mail: kwwang@umich.edu

The ORCID identification number(s) for the author(s) of this article can be found under https://doi.org/10.1002/adma.201805282.

ADVANCED
SCIENCE NEWS
www.advancedsciencenews.com

ADVANCED
MATERIALS
www.advmat.de

material properties. This is because we can both "program" the properties by custom designing the underlying crease pattern (before folding), and "tune" them on-demand by folding to different configurations. Moreover, the principle of folding is scalable, which makes it possible to achieve desired material properties at vastly different sizes (see examples in Figure 1).

In addition to promoting the origami mechanics research, the efforts of developing architected origami materials are starting to foster a synergy between the different branches of origami research, including the mathematical theories of crease design, mechanics analysis of folded structure, and advanced fabrication through folding. These branches have been evolving relatively independently over the last several decades; however, origami materials is a unique topic that requires a tight integration of all these branches so it provides an opportunity to mature the vibrant field of origami research as a whole.

Therefore, the architected origami materials is a transformative topic that can lead to the next evolution in mechanical metamaterials and applied origami, and many relevant literatures have been published recently. There are several excellent review papers in origami, however, they focused on the design,[40,41] kinematics,[10,12] self-folding,[11] fabrication,[28,42] and specific applications like robotics.[43] There is a need to specifically report the recent progress in *architected origami materials* and the *mechanics* of folding. Therefore, in this paper we review the design strategies, mechanics analysis methods, unique mechanical properties, and the advanced fabrication techniques regarding origami materials. We also discuss the challenges and future research topics that are critical to flourishing and maturing this promising field.

It is worth noting that the definition of origami can been broadened. We mostly focus here on architected materials based on origami in the traditional sense, that is, the origami consists of creases with highly concentrated deformation and facets with relatively small or no deformation during folding. Meanwhile, several studies have proposed a broader definition: that is, origami can be regarded as any approach to create 3D shapes by inducing out-of-plane deformations in sheet materials.[44–48] Such generalized origamis can be made of relatively soft materials, and they do not necessarily show any sharp distinctions between creases and facets. Discussions on such generalized origamis, however, are beyond the scope of this report.

2. Strategies for Constructing Materials Using Origami

Origami designs for art and architecture are exceptionally rich,[1] however, designing the folding pattern for building architected materials has a completely different set of priorities and constraints. Conventional origami art design usually considers three different geometric characteristics: The first one is the *developability*, meaning that origami can be developed from folding a flat sheet. For a simple degree-4 vertex where four crease lines meet, being developable means that the four corresponding sector angles between adjacent creases can sum

Suyi Li is an assistant professor of mechanical engineering at the Clemson University. He received his Ph.D. at University of Michigan in 2014. After spending two additional years at Michigan as a postdoctoral research fellow, he moved to Clemson in 2016 and established a research group on dynamic matters. His technical interests are in origami-inspired adaptive structures, multifunctional mechanical metamaterials, and bioinspired robotics.

Hongbin Fang has been an associate professor in the Institute of AI and Robotics at Fudan University since 2018. He received his Ph.D. from Tongji University in 2015. Prior to his current position, he worked as a postdoctoral research fellow at the University of Michigan (2015 to 2017) and at the Hong Kong Polytechnic University (2017–2018). Fang's technical interests are in origami-inspired mechanical metamaterials, bioinspired robotics, nonlinear dynamics, and control.

Kon-Well Wang is the Stephen P. Timoshenko Professor of mechanical engineering at the University of Michigan since 2008. He received his Ph.D. from the University of California at Berkeley in 1985, worked at the GM Research Labs, and started his academic career at the Pennsylvania State University in 1988. Wang's technical interests are in adaptive structures and structural dynamics via exploring emerging areas such as piezoelectric circuitry networks, metastable metastructures, and origami and cellular-composites.

up to 360° (aka $\theta_A + \theta_B + \theta_C + \theta_D = 360°$ in **Figure 2**a). The second characteristic is *flat-foldability*, meaning that origami can be fully folded into another flat configuration (assuming zero sheet thickness). For a degree-4 vertex, this requires $\theta_A - \theta_B + \theta_C - \theta_D = 0$ according to the Kawasaki's theorem.[2,7] When both developability and flat-foldability are desired, one can impose $\theta_A = 180° - \theta_C$ and $\theta_B = 180° - \theta_D$. The third characteristic is *rigid-foldability*, meaning that origami can fold

ADVANCED
SCIENCE NEWS
www.advancedsciencenews.com

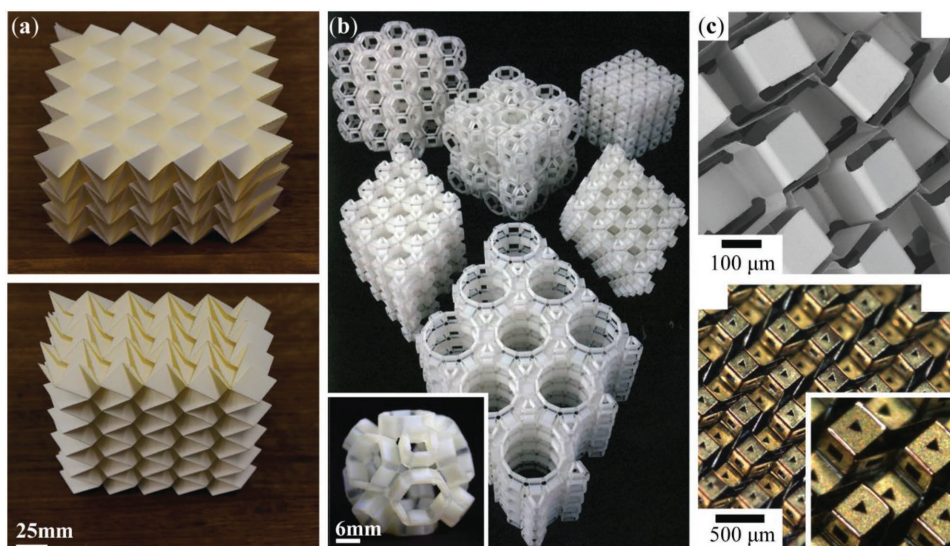**ADVANCED**
MATERIALS
www.advmat.de

Figure 1. The wide variety of architected origami materials at different length scales. a) The stacked Miura-ori material proposed by Schenk and Guest is one of the well-studied examples. b) A 3D printed, prismatic material consisting of foldable modules (one shown in the insert). c) A smaller scale material based on the chess board pattern, which involves both folding and cutting (aka Kirigami). a) Reproduced with permission.[32] Copyright 2013, National Academy of Sciences. b) Reproduced with permission.[49] Copyright 2017, The MIT Press, Springer Nature Limited. b-inset) Reproduced with permission.[50] Copyright 2017, The MIT Press, Springer Nature Limited. c) Reproduced with permission.[51] Copyright 2009, American Institute of Physics.

without inducing any facet deformations. That is, origami can fold smoothly even if the facet material is assumed rigid and rotating around the hinge-like creases (folds). Rigid-folding can be described by kinematic equations based on spherical trigonometry.[52–54] For example, for a degree-4 vertex

$$\cos \rho_{AB} = \cos \rho_{BC} + \frac{\sin^2 \rho_{BC} \sin \theta_A \sin \theta_B}{1 - \cos \xi} \qquad (1)$$

where ρ_{AB} and ρ_{BC} are the dihedral *crease folding angles* between adjacent facets (Figure 2a), and the angle ξ is defined as
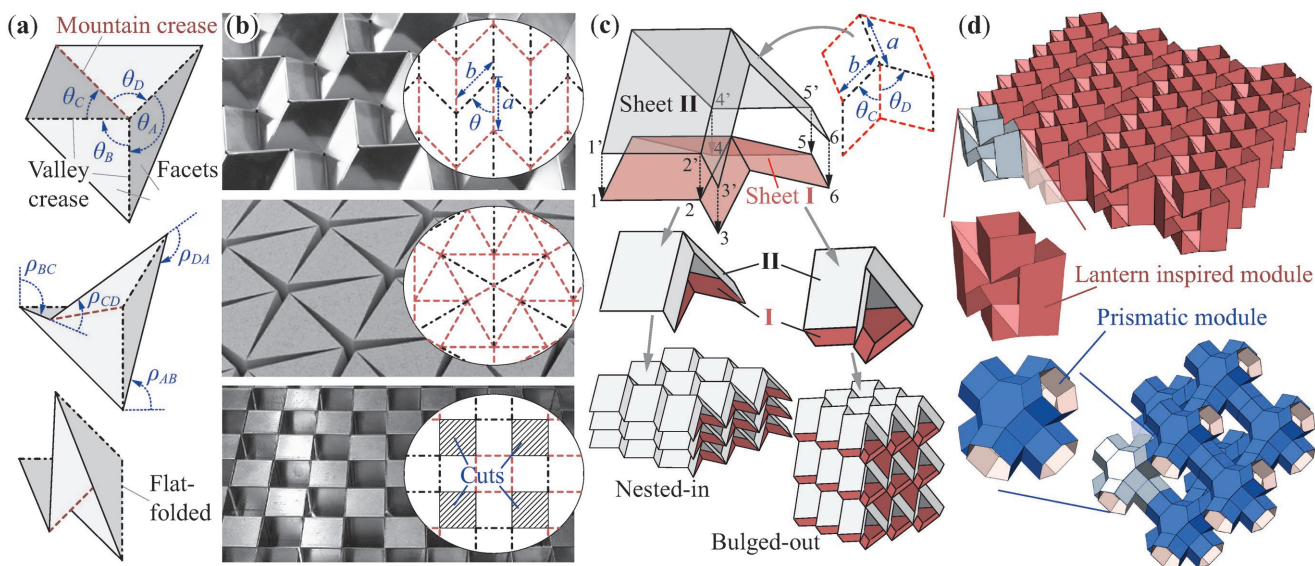

Figure 2. Different design strategies for constructing the architected origami materials. a) A generic flat-foldable degree-4 vertex showing the definition of sector angles θ_i and dihedral crease folding angle ρ_{ij}. b) Single origami sheet used as sandwich core materials. The three examples are (from the top): classic Miura-ori consisting of degree-4 vertices, a Ron-Resch pattern consisting of degree-6 vertices, and a chess board pattern involving some Kirigami cutting. b-top) Adapted with permission.[32] Copyright 2013, National Academy of Sciences. b-middle) Adapted with permission.[60] Copyright 2013, American Society of Mechanical Engineers. b-bottom) Adapted with permission.[61] Copyright 2007, Springer Nature Limited. c) Stacking generic flat-foldable origami sheets showing the nested-in and bulged-out configurations. Adapted with permission.[62] Copyright 2016, American Physical Society. d) Assembling foldable modules. The example above is a Chinese lantern inspired design, and below is a rational prismatic design. Lantern-inspired module: Adapted with permission.[63] Copyright 2017, National Academy of Sciences. Prismatic design: Adapted with permission.[50] Copyright 2017, Springer Nature Limited.

$$\cos \xi = -\cos \theta_A \cos \theta_B - \sin \theta_A \sin \theta_B \cos \rho_{BC} \qquad (2)$$

While the aforementioned geometric characteristics are often desired in the origami design for art and architecture, they are not all necessary for constructing architected materials. For example, flat-foldability and rigid-foldability can be intentionally violated to create desirable material properties (to be detailed in Section 4). On the other hand, spatial periodicity (aka tessellation) are normally required or desired in the crease pattern to effectively provide homogenous material properties. Moreover, additional geometric constraints are needed to assemble folded origami sheets and modules. Here, we discuss several commonly used strategies of designing and constructing materials using origami.

2.1. Leveraging a Single Origami Sheet

A single piece of folded origami sheet can be directly used as an architected material (Figure 2b). It is typically used as a sandwich core (aka "foldcore") so its out-of-plane properties are of primary interest. The most well-studied example is the Miura-ori sheet, proposed by Koryo Miura back in the 1970s,[55] which consists of simple 4-vertices with $\theta_C = \theta_D = \theta$ and $\theta_A = \theta_B = 180° - \theta$. Origamis consisting of higher order vertices like the Waterbomb[56] base and Ron-Resch[34] pattern were also examined. Their folding are more complicated than the Miura-ori, but can impart many unique properties. Besides folding, additional cutting (aka Kirigami) can significantly enrich the design space and create geometries that are very difficult to achieve just by folding, like the hexagon sandwich and chess board pattern.[57–59]

2.2. Stacking Multiple Origami Sheets

Due to their spatial periodicity, folded origami sheets can be naturally stacked and assembled together to form a space-filling topology. In this way, one can design material properties along all three principle axes in space. Some of the earliest examples using this approach are the stacked Miura-ori[32] and Tachi–Miura polyhedron (TMP).[64] These stacked origamis are particularly interesting in that they remain developable, flat-foldable, and rigid-foldable, so that many material properties from a single origami sheet are retained in the stacked system. While stacking identical origami sheets is relatively straightforward, stacking sheets with different designs requires elaborate geometric constraints to ensure that they do not separate from each other during rigid-folding. For example, when stacking two different sheets consisting of generic flat-foldable 4-vertices (Figure 2c), crease lines that are shared by the two sheets should have the same length (aka $\overline{12} = \overline{1'2'}$, $\overline{23} = \overline{2'3'}$, etc.); the distance between these connecting creases should be equal throughout the range of rigid-folding ($\overline{36} = \overline{3'6'}$, $\overline{25} = \overline{2'5'}$, etc.); and the angles between them should also be consistent ($\angle 123 = \angle 1'2'3'$). By incorporating the rigid-folding kinematics, the following crease design constraints can be derived[62]

$$b^I = b^{II} \text{ and } \frac{a^I}{a^{II}} = \frac{\cos \theta_C^{II}}{\cos \theta_C^I} = \frac{\cos \theta_D^{II}}{\cos \theta_D^I} \qquad (3)$$

where the super indices I and II represent the two sheets. Stacked origami sheets can be folded into two different types of configurations. In one type, the smaller sheets are "nested-in" the larger sheets; while in the other type, the smaller sheets are "bulged-out" (Figure 2c). The overall material property can be fundamentally different between these two configurations (to be detailed in later sections).

2.3. Assembling Foldable Modules

Another powerful approach for constructing architected origami material is by assembling foldable modules like tubular bellows,[65–67] prismatic polyhedron,[50,68] or Kirigami units[63] (Figure 2d). This approach is inspired by the art of "modular origami." Here, a single module is constructed by a combination of folding, cutting and gluing thin sheets, so it is topologically different from a folded origami sheet. The modules need to be carefully designed with periodic features for a successful assembly. A key advantage of such module-based materials is that they can exhibit more isotropic material properties than the stacked origami sheets because a module can be designed to be highly symmetric (e.g., the prismatic module in Figure 2d). Moreover, the modular origami materials can possess more than one degree-of-freedom (DOF) for rigid-folding with sophisticated shape transformations,[68] while the stacked origami sheets typically have only one DOF.

It is worth highlighting that the sheet stacking and module assembling approach do not fully constrain the constituent origami designs. That is, the number of origami design variables exceeds the number of geometric constraints from stacking or assembly, so that we still have much freedom to tailor the shapes and properties of origami materials.[63,65,69–71] This fundamental principle ensures their potentials for practical applications with vastly different requirements.

3. Analytical Tools for Origami Mechanics

Mechanics models of origami are the catalysts and analytical foundations for synthesizing architected origami materials, and they were used extensively to analyze the mechanical properties covered in this report. Here, we categorize the currently available models into three different categories based on their complexities: They are the rigid-facet, lattice framework, and the finite element approaches. The fundamental difference among these three approaches is their assumptions on facet deformation. When under external loads, the origami facets can exhibit very complex deformations including bending, twisting, and stretching; however, it is often necessary to make some assumptions in the analytical model to reveal the underlying physical principles without unnecessary complexities. The rigid facet approach assumes negligible facet deformation; the lattice approach allows a simple bending in the facets; while the finite element approach does not impose any explicit simplification. Each approach has its unique balance between analytical capability and computational cost and they are discussed in detail below.
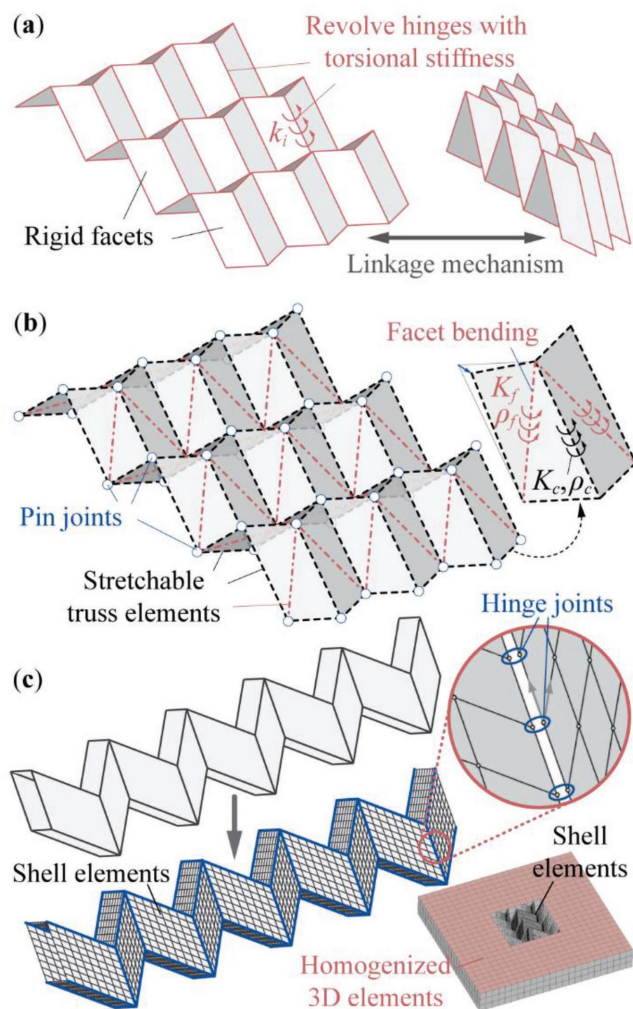
Figure 3. The different approaches to analyze origami mechanics. a) Rigid-facet approach, where k_i is the torsional stiffness coefficient of the hinge-like creases. b) Lattice framework approach. The assigned torsional stiffness for characterizing facet bending (K_f) and crease folding (K_c) are highlighted. c) Finite element approach, showing the hinged joints with assigned torsional stiffness for modeling the creases. c) Adapted with permission.[16] Copyright 2015, National Academy of Sciences. Lower right: A hybrid model of a Miura-ori sheets consisting of shell element meshing and equivalent 3D elements with homogenized property. Adapted with permission.[78] Copyright 2013, Springer Nature.

3.1. Rigid-Facet Approach

This approach leverages the rigid-foldable characteristics of certain crease designs and assumes that the facet is rigid and the crease behaves like a hinge. In this way, origami folding is achieved by facets revolving around the creases like a planar linkage mechanism (**Figure 3**a). Under this assumption, the admissible degree of freedom in origami deformation is limited to rigid folding. For example, for a rigid-foldable 4-vertex like the Miura-ori, the corresponding mechanics model has only one degree of freedom. Using this approach, one can easily analyze the *kinematics* of rigid folding and the corresponding deformation pattern of the architected origami materials by using spherical trigonometry (e.g., Equation (1)). This is particularly

powerful for predicting their auxetic properties (aka negative and flipping Poisson's ratio).[32,62,72]

The rigid facet approach also offers the most simple route to incorporate the elastic potential energy of folding: One can assign torsional stiffness to the hinge-like creases so the total potential energy of the origami material is a summation of its spring energies at the creases: $\Pi = \sum_i k_i (\rho_i - \rho_i^o)^2 / 2$, where the subindex i represents the different creases in the origami, k_i is the corresponding torsional stiffness coefficient, and ρ_i^o is the initial rest angle. In addition to using the crease folding angles (ρ_i), one can also derive the total energy based on the vectors along creases and facets.[73] The effective reaction force of the architected origami material due to a prescribed deformation (dx) can then be calculated using the virtual work principle so that

$$F = -\frac{d\Pi}{dx} = -\sum_i \left[k_i \left(\rho_i - \rho_i^o \right) \left(\frac{dx}{d\rho_i} \right)^{-1} \right] \tag{4}$$

The elastic property of the architected origami material is strongly nonlinear due to the intricate relationships between folding ($d\rho_i$) and external dimension change (dx). Moreover, the rest angle (ρ_i^o) also plays an important role. Typically, an origami sheet is at rest before it is folded (aka at the flat configuration with $\rho_i = 180°$); however, tailoring this rest angle can open up new opportunities for material property programming. Although seemingly simple, the rigid facet approach with assigned crease torsional stiffness directly correlates the folding kinematics to the mechanical properties; therefore, it can reveal many interesting material behaviors like the multistability.[73–75]

The rigid facet approach can be extended to nonrigid foldable origamis by carefully adding "virtual folds" to the facets, which essentially add additional degrees of freedom to the mechanics model to accommodate the non-negligible facet deformation during folding. For example, the bistable nature of a nonrigid foldable square twist pattern can be analyzed by placing a virtual fold across the diagonal of its center square facet.[76] The additional configuration space obtained by adding virtual folds to a generic 4-vertex origami reveals a "diodic" behavior that can be exploited to create mechanical robustness.[77] However, due to its simplicity, the rigid facet approach can only provide qualitative analyses.

3.2. Lattice Framework Approach

This approach transforms the continuous origami sheets into an equivalent lattice system by using stretchable truss elements to represent the crease lines and pinned joints for vertices. Additional truss elements are added to the quadrilateral facets to describe their deformations. Torsional stiffness are assigned to the dihedral angles between two adjacent triangles defined by five truss elements, either along the creases or across the facets (K_c and K_f in Figure 3b, respectively). In this way, the lattice system can not only characterize the crease folding but also consider simple facet bending and stretching, making it fundamentally more capable than the rigid facet approach.

Several methods of constructing the mechanics model based on lattice framework have been derived,[77,79–82] but their

**ADVANCED
SCIENCE NEWS**

www.advancedsciencenews.com

**ADVANCED
MATERIALS**

www.advmat.de

underlying principles are similar. Here we discuss the one used by Guest et al.[32] and Li et al.[83] as an example. Denoting $\mathbf{x}$ as the vector of current vertices positions and $d\mathbf{x}$ as the vector of infinitesimal vertices displacements, the correlation between $d\mathbf{x}$ and the longitudinal stretches of the truss element ($\mathbf{e}$) can be described by a linear matrix equation $\mathbf{C}d\mathbf{x} = \mathbf{e}$, where the *compatibility matrix* $\mathbf{C}$ is a function of $\mathbf{x}$ and hence the folding configurations.[79,84] One can derive another linear matrix equation $\mathbf{J}_c d\mathbf{x} = d\boldsymbol{\rho}_c$, where $\mathbf{J}_c$ is a transformation matrix correlating the vertices displacements to the infinitesimal changes in crease folding angles.[79] Similarly, one can construct $\mathbf{J}_f d\mathbf{x} = d\boldsymbol{\rho}_f$ for the angles of facet bending ($d\boldsymbol{\rho}_f$). The total stiffness matrix $\mathbf{K}$ of the origami lattice is the summation of three components including the truss stretch stiffness $\mathbf{K}_t (= \mathbf{C}^T \mathbf{G}_t \mathbf{C})$, crease torsional stiffness $\mathbf{K}_c (= \mathbf{J}_c^T \mathbf{G}_c \mathbf{J}_c)$, and facet bending stiffness $\mathbf{K}_f (= \mathbf{J}_f^T \mathbf{G}_f \mathbf{J}_f)$, where $\mathbf{G}_t$, $\mathbf{G}_c$, and $\mathbf{G}_f$ are diagonal matrices containing the equivalent stiffness coefficients of the trusses, creases, and facets, respectively.[16] The magnitudes of these stiffness coefficients need to be estimated carefully based on the facet geometries and constituent material properties.[85] It is worth emphasizing that the lattice formulation discussed above is only suitable for analyzing small deformations. The truss elements can be replaced with frame elements that feature not only stretching but also bending degrees of freedom.[86] Nonlinear lattice formation were also developed to analyze large amplitude deformations.[87,88]

Compared to the rigid facet approach, the additional degrees of freedom in the lattice approach enable us to analyze origami deformation beyond rigid-folding. For example, the null space of compatibility matrix $\mathbf{C}$ (aka the configuration space of lattice) contains vertex deformations that do not induce any truss element stretching so it can reveal the "soft modes" of origami, which is the deformation patterns with the least resistance to external force. For example, the null space of $\mathbf{C}$ of a single Miura-ori sheet, assuming periodic boundary conditions, has a rank of three corresponding to rigid-folding, bending, and twisting motion, respectively.[79] However, when multiple Miura-ori are stacked, the rank of its null($\mathbf{C}$) dropped to 1 corresponding to rigid folding only.[83] This means that the stacked Miura-ori sheets are fundamentally stiffer than a single sheet against bending and twisting.

In addition to configuration space study, eigenvalue analysis based on the lattice stiffness matrix provides deeper insights into the origami mechanics. For example, it is used to analyze how an increase in facet bending stiffness relative to the crease torsional stiffness can influence the "softest" modes of a single Miura-ori sheet. Results show that it is easier to bend and twist a Miura-ori sheet than to fold it, unless the facet bending stiffness is significantly higher than the creases torsional stiffness.[79] Eigenvalue analysis can also reveal how the stiffness of different deformation modes changes with respect to folding configurations. Inhomogeneous deformation such as the edge deformation due to an indenter or the internal frustration due to a pop-through defect (PTD) can be analyzed by the lattice frame model as well.[80]

The lattice approach is also powerful for predicting the deformation of nonrigid-foldable origami. For example, the bistability of the Kresling pattern can be analyzed by the truss frame approach, where the complex crease warping occurring between the two stable states can be characterized by the extension and shrinking of certain truss elements.[89]

Despite these capabilities, obtaining a quantitative accuracy between analytical prediction and experimental results is still a challenge for the lattice frame approach. This is due to the limitation of assuming simple bending in facets and representing the constitutive properties of a continuous sheet by discrete lattices. To obtain an accurate analytical prediction or to analyze more complex facet deformations, finite element approach is preferred.

3.3. Finite Element Approach and Homogenization

Since the thickness of folded sheets are small compared to the overall size of origami material, facets are typically meshed by different types of shell elements in the finite element method.[72,90–95] Modeling the creases on the other hand is not a trivial task because the material stiffness and strength along the crease can be lower than the facets due to fabrication. That is, the raw sheet materials are intentionally thinned to create the crease pattern, and folding can further weaken the crease material. Two different methods of modeling creases have been implemented so far. One is to use additional hinge connection elements to join the overlapping shell element nodes that are on the creases, and assign linear torsional stiffness to these hinges just like in the aforementioned rigid-facet and lattice frame approaches (Figure 3c).[16,72,96] The other method is to use a refined mesh near the creases and assign reduced stiffness and strength properties to them.[95] The finite element model can be used to perform eigen analysis to accurately analyze the deformation modes of origami materials and validate the results from the lattice approach.[16] Moreover, localized and irreversible deformations in the facets, such as the buckling and crushing due to impacts, can be examined with detail (Section 4.5). It is worth noting that the finite element approach is also used to analyze the more generalized origami discussed in Section 1.[44,48]

Although accurate and capable, finite element simulation can lead to a very high computational cost. A promising solution to address this issue is to create a hybrid model. In this model, detailed shell element mesh is applied only to parts of the origami material where localized deformations like buckling and crushing are expected; while other parts of the material are replaced by customized 3D elements with homogenized properties (Figure 3c, lower right).[97] Deriving homogenized models for the origami material is still an open research problem and only a few attempts has been published so far based on Miura-ori. For example, by imposing a uniform stress and strain to the unit cell of a Miura-ori and calculating the corresponding elastic energy, the lower and upper bound of its effective shear stiffness were derived, respectively.[98] This homogenization was improved further by incorporating a bending-gradient plate theory.[99] Another method of obtaining homogenized property was to directly use the result of finite element simulation.

4. Folding Induced Mechanical Properties

The intricate geometries created by folding, together with the new origami mechanics models, open up many opportunities
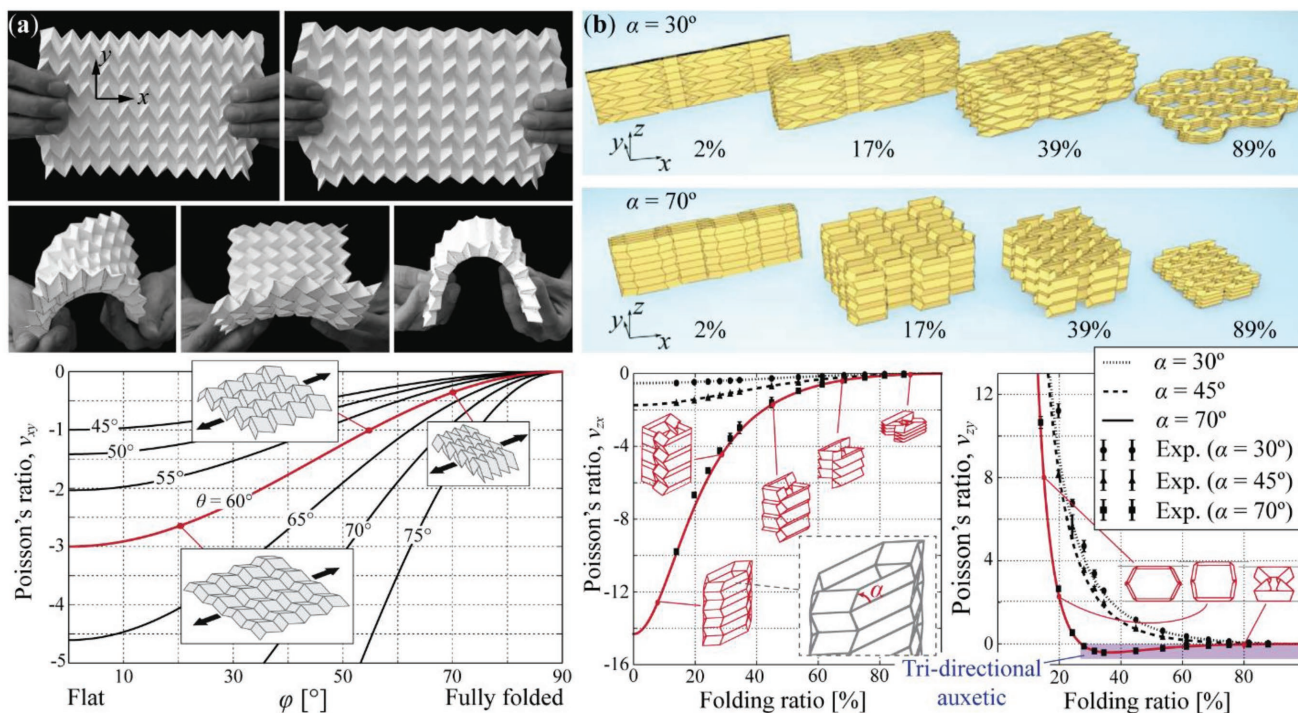
Figure 4. Auxetic properties of the architeced origami materials. a) Top: the in-plane and out-of-plane deforamtion of a Miura-ori sheets show a pecurliar combination of negatve and positive Poisson's ratio. Bottom: The value of the in-plane negative Poisson's ratio is directly related to the Miura-ori design and folding. Top images: adapted with permission.[79] Copyright 2011, National Academy of Sciences. Bottom graph: adapted with permission.[32] Copyright 2013, National Academy of Sciences. b) Top: Possion's ratio of reentrant origami materials based on different variations of Tachi-Miura Polyhedron (TMP). Below: with certain designs and folding configurations, this material shows auxetic behavior along all three axes (hightlighted). Adapted with permission.[66] Copyright 2010, American Physical Society.

for constructing architected materials with desirable and even unorthodox properties. This section surveys the different material properties that have been achieved so far. Especially, we emphasize how the material properties can be programmed via designing the origami crease pattern and tuned on-demand via folding.

4.1. Shape Reconfiguration and Auxetic Properties

The deformation pattern of the architected origami materials is dictated by the kinematics of folding, which offers the route to achieve prescribed shape reconfigurations[68] and auxetic properties (aka negative Poisson's ratio). The latter is indeed one of the first properties that were investigated in origami materials. For example, the classical Miura-ori sheet exhibits a negative Poisson's ratio in plane. That is, when it is stretched along x or y-coordinate as shown in **Figure** 4a, it will expand in the direction perpendicular to the external load direction. Such an auxetic behavior originates solely from the spatial re-orientations of facets and creases according to the rigid-folding kinematics, so that the Poisson's ratio can be calculated accurately based on the rigid-facet approach (without assigning crease torsional stiffness)

$$v_{xy} = -\frac{\varepsilon_y}{\varepsilon_x} = -\tan^2\theta\cos^2\varphi \qquad (5)$$

where θ is the sector angle shown in Figure 2b and ϕ is the dihedral angle between the x–y reference plane and facets.[32,33]

Here θ and ϕ can take any values between 0 and 90° so that the absolute magnitude of negative Poisson's ratio can be very large if the sector angle of Miura-ori is big ($\theta \to 90°$) and it is folded close to a flat configuration ($\phi \to 0°$) Figure 4a. The same Miura-ori sheet, on the other hand, exhibits a saddle shape when it is bent out-of-plane, indicating a positive out-of-plane Poisson's ratio. Such a peculiar combination of negative and positive Poisson's ratios is not available from any monolithic materials.

When Miura-ori sheets with different but compatible designs are stacked together, the Poisson's ratio along x and y-axes (v_{xy}) has the same negative magnitude as the constituent single sheets. However, the Poisson's ratios along z-axis (v_{xz} and v_{yz}) can flip their sign depending on the folding configuration: They are positive when the smaller Miura-ori is bulged-out of the bigger sheets (Figure 2c), and negative when the smaller Miura-ori is nested-in so that the stacked Miura-ori becomes auxetic along all three axes (tridirectional auxetic). The auxetic properties of origami materials can be further enriched by tailoring the underlying crease patterns. For example, a rigid-foldable sheet consisting of more generic flat-foldable 4-vertices can exhibit a flip of its out-of-plane Poisson's ratio between positive and negative even without stacking.[62] Using a parameterized curve-like fold pattern[72] or a zig-zag folding with cut openings[100] can give a richer design space to program the auxetic properties. Besides single origami sheet and stacked sheets, foldable modules used in many origami materials also exhibit negative Poisson's ratio (an example shown in Figure 4b).[50,63,67,101] Indeed, auxetics is near ubiquitous among the rigid-foldable origamis.

4.2. Nonlinear and Tunable Stiffness

Folding is an intricate yet predictable mechanism to spatially arrange facets and creases so it can open up exciting possibilities to achieve nonlinear and tunable stiffness. Due to the interleaved nature of facets, the architected origami materials are essentially close-walled cellular solids, and they can be divided into two categories according to their folding kinematics. The first category is based on rigid-foldable origamis that have at least one degree of freedom to fold without inducing any facet deformations. Therefore, the stiffness of these materials can be tuned by folding on-demand, and they can accommodate additional mechanisms for stiffness control such as fluidics. The second category of origami material is based on nonrigid foldable origamis that rely on facet or crease deformations to fold, so that typically they exhibit higher stiffness to density ratio. In this subsection, we review the stiffness characteristics of these two categories of materials. Then we further discuss a self-locking origami material that essentially integrates the advantages of these two categories.

Origami Materials Based on Rigid-Foldable Designs: These architected materials are constructed using rigid-foldable origami patterns such as Miura-ori[32,79] and TMP.[64] Their stiffness properties are dictated by the spatial arrangements of facets and creases, and rigid folding offers the freedom to effectively change their orientations. Therefore, one can tune the stiffness of such origami materials significantly by on-demand folding. Indeed, this stiffness tuning capability is one of the fundamental advantages of architected origami materials compared to other mechanical metamaterials. Several eigenvalue studies have been conducted to uncover this correlation between folding and stiffness properties. In one study, single Miura-ori tube and "zipper-coupled" tube assembly were examined by using the equivalent truss-frame approach. This study showed that the eigenvalues of different modes of deformation is quite sensitive to folding, and there is an eigenvalue "bandgap" between the softest mode of folding and other modes of more complex deformations (**Figure 5**a).[16] This bandgap narrows significantly near the fully folded and unfolded configurations, but the zipper coupling can significantly widen it. Another eigenvalue study investigated the *homogeneous* deformation patterns and anisotropic stiffness of a stacked Miura-ori material.[83] This study showed that the stacked Miura-ori exhibits a strong stiffness anisotropy, which is also coupled to rigid-folding. Other than eigenvalue analyses, experimental and finite elements approaches were used to investigate the stiffness versus folding relationships of a TMP bellow assembly[64] and 3D printed origami inspired building blocks.[101]

Rigid-foldable origami materials can also accommodate the use of fluidic pressure to actively tailor their stiffness properties. Many architected origami materials, such as the stacked Miura-ori, have naturally embedded tubular channels that can be pressurized by fluidic principles (aka fluidic origami). The nonlinear relationships between the internal enclosed volume and external deformation can be exploited to achieve pressure induced stiffness control,[83] rapid shape reconfiguration,[102] recoverable and programmable collapse[103] (Figure 5b), and quasi-zero stiffness properties.[104]

Origami Materials Based on Nonrigid Foldable Designs: These materials can be constructed either by directly using nonrigid foldable crease patterns, or by combining rigid-foldable but kinematically incompatible patterns. Since rigid-folding is no longer admissible, the facets would carry most of the external loads. The nonrigid foldable origami materials therefore lose the aforementioned capability of stiffness tuning by folding, but they exhibit relatively higher stiffness to density ratios. It was shown that by carefully designing the geometry and using well distributed networks of facets to transfer load efficiently, it is even possible to reach the Hashin–Shtrikman upper bounds on isotropic elastic stiffness.[106]

The most well-studied example of nonrigid foldable origami materials is the *foldcore* consisting of a Miura-ori sheet bonded to two flat face skins.[78,90,107] This material was initially proposed as an alternative to the honeycomb and technical foam for aircraft applications, because it features open ventilation channels that can avoid the moisture accumulation issue. Via experiment testing and finite element simulations, foldcore materials are shown to exhibit a desirable combination of high bending and shear stiffness,[90,95] impact absorption (to be detailed later), and low effective density. The foldcore further evolved to feature curved folding pattern and multiple layer stacking, which yield a bending stiffness comparable to the honeycomb core.[91]

Another example of nonrigid foldable origami materials is the interleaved materials consisting of rhombic dodecahedron unit cells.[108] This material is constructed by assembling rigid-foldable origami tubes and their affine transformations in an interleaved pattern, so that these two types of tubes are spatially orthogonal to each other. Such arrangement creates a statically over-constrained system so that the material is quite stiff in one direction with a desirable stiffness-density scaling relationship.

Self-Locking Origami Materials with Discrete Stiffness Jump: When self-locking occurs, the origami will be "stuck" at a particular configuration and cannot be folded further. There are various mechanisms that can induce locking such as non-negligible facet thickness,[15] locking elements,[109,110] and active materials.[111,112] Self-locking is an interesting mechanism for the origami materials because it combines the characteristics of rigid-folding and nonrigid folding. That is, locking acts like a phase transition from a state where the origami is rigid-foldable to a state where it is no longer rigid-foldable.

Self-locking in the origami materials can be achieved by using nonflat foldable vertices, whose facets can come into contact before being folded into a fully flat configuration (aka facet binding).[77] The early study by Schenk and Guest showed that using a nonuniform Miura-ori crease pattern can ensure that a stacked origami material is locked in a predetermined configuration.[32] Fang et al. extended the study by using generic 4-vertices, and identified several different self-locking mechanisms that involves facet-binding either within constituent origami sheets or between adjacent sheets.[62,113] They further examined the locking-induced discrete stiffness jumps using both numerical simulations and experiments.[105] Before locking occurs, origami deforms by following the kinematics of rigid-folding so the effective material stiffness comes primarily from the crease torsional stiffness. After self-locking (or facet binding), origami cannot be rigid-folded anymore and facet will instead directly
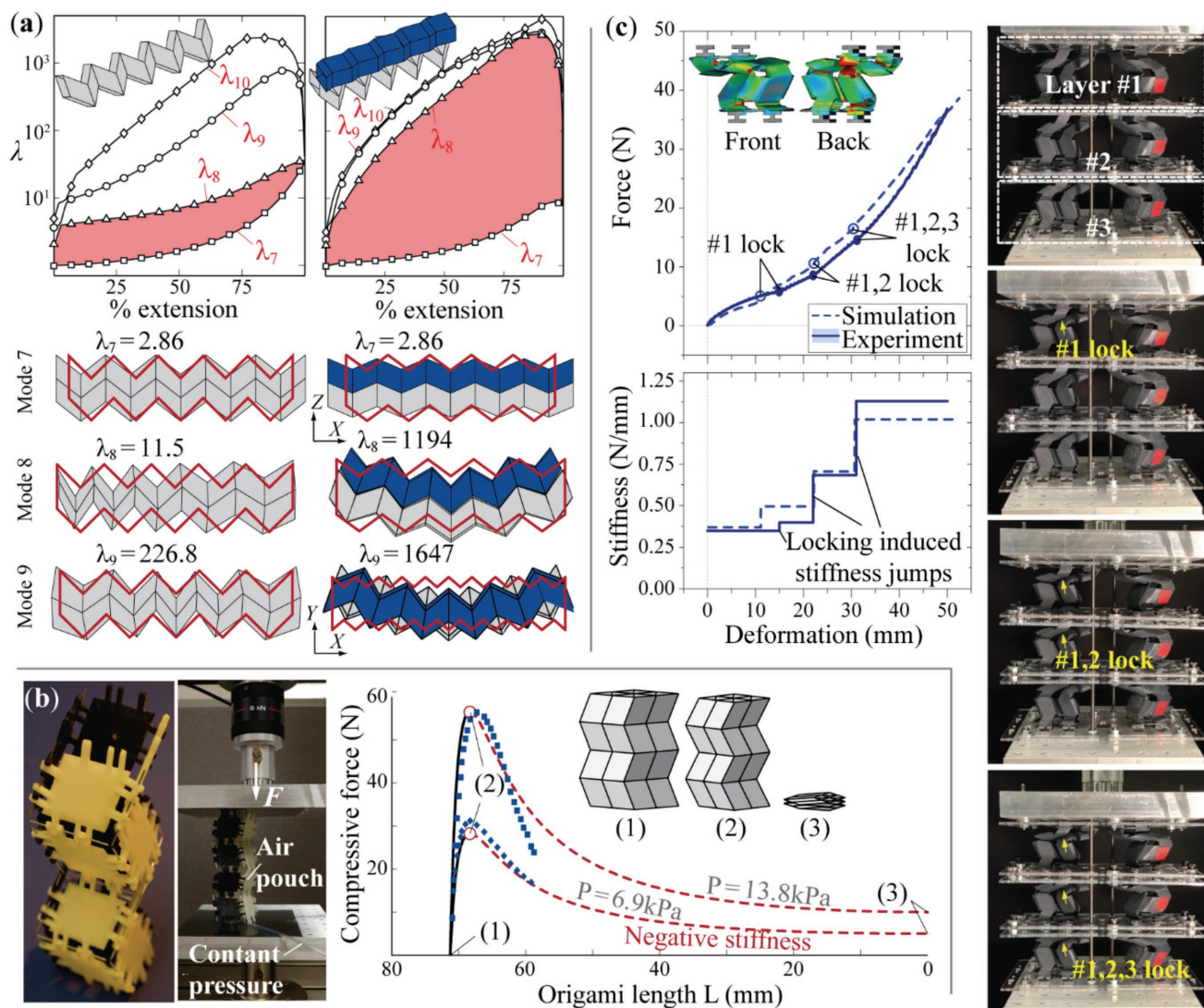
Figure 5. Tunable stiffness properties of architected origami materials. a) Eigenvalue analysis of the rigid-foldable Miura-ori tube and "zipper-tube" assembly demonstrates how the eigenvalues of different modes of deforamation evolve with respect to folding. Adapted with permission.[16] Copyright 2015, National Academy of Sciences. Here λ_i are the eigenvalues corresponding to differet deformation modes. Mode 7 is the folding deformaiton, and Modes 8–10 are more complicated deformation. b) Fluidic principle applied to stacked Miura-ori can induce desirable nonlinear stiffness properties like the recoverable collapse via rigid-folding. The reaction force at collapsing can be tuned by controlling internal pressure. Adapted with permission.[103] Copyright 2016, American Physical Society. c) Programmed and progressive self-locking in stacked single-collinear origami can introduce discrete stiffness jumps and create piecewise linear stiffness profile. Adapted with permission.[105] Copyright 2018, Wiley-VCH.

carry the external load, leading to a much higher stiffness. Based on this principle, one can derive a method to program a piecewise linear stiffness profile using single-collinear 4-vertices (Figure 5c). A graded stiffness was also achieved by the self-locking principle.[114]

4.3. Multistability

An origami is considered to be multistable when it possesses more than one stable equilibria (or stable states), and can remain in any one of these states without external aids. Such unique property, which can be characterized by the multiple potential energy minima with respect to folding (**Figure 6**a),

is a result of the nonlinear correlations between folding and crease/facet material deformations. Multistable origami can exhibit many unique behaviors. For example, they can generate a rapid "snap-through" response and negative effective stiffness when passing through the critical, unstable equilibrium during folding. They can also re-configure themselves into different designated shapes. These behaviors, coupled with the aforementioned tunable stiffness and auxetic properties, can become the catalyst for synthesizing new material properties. Similar to the previous subsection, the underlying mechanisms to achieve multistability can also be divided into two categories: rigid-foldable and nonrigid foldable. In the following subsections, we survey the different multistable origamis in conjunction with their potential applications as architected materials.
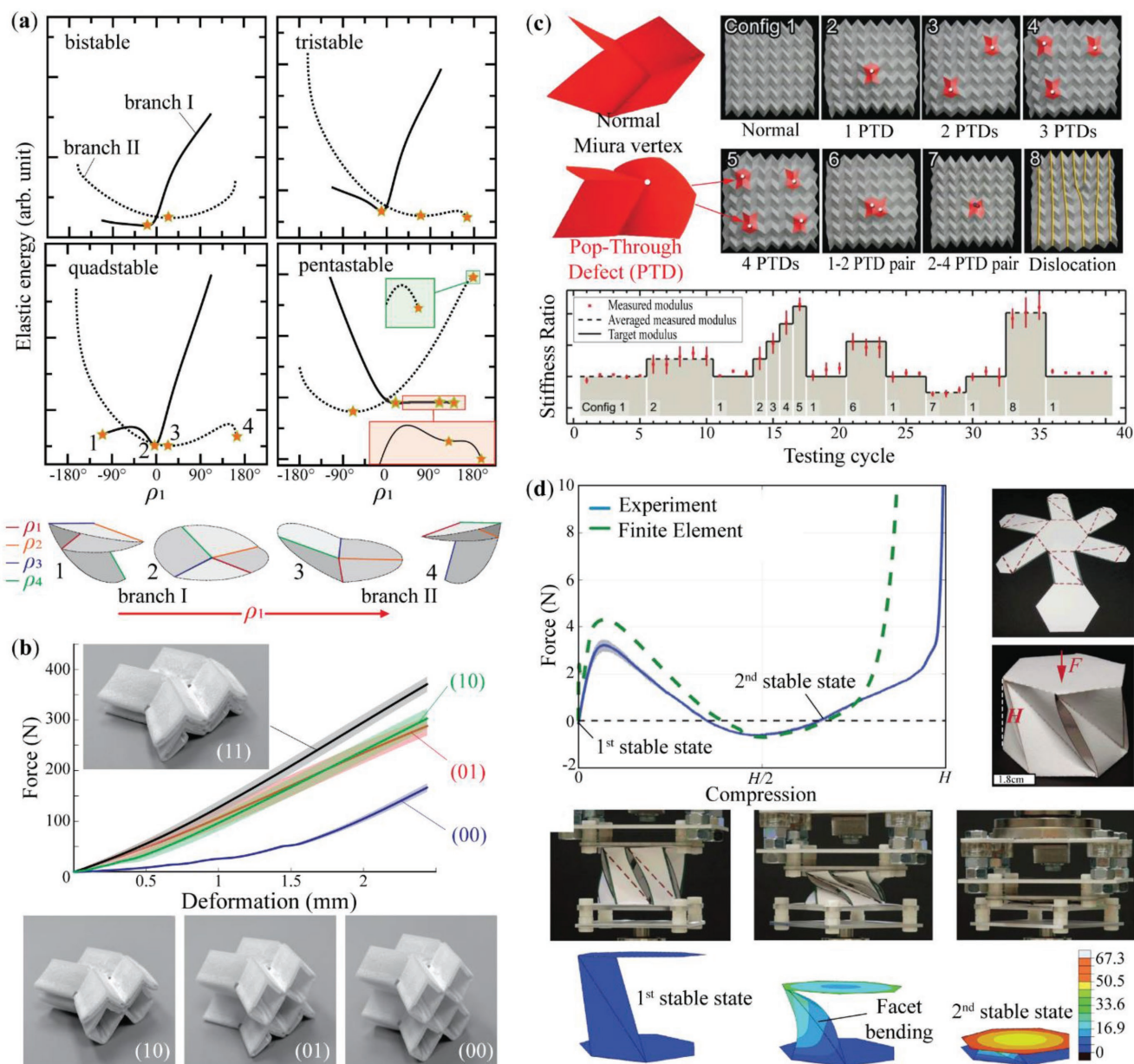
Figure 6. Multistability of architected origami materials. a) Rigid-foldable, generic degree-4 vertices can be strongly multistable via tailoring its sector angles, crease torsional stiffness, and the rest angles. Reproduced with permission.[74] Copyright 2015, American Physical Society. b) Stacked Miura-ori sheets with different crease stiffness can be multistable via rigid-folding, leading to programmable modulus. Adapted with permission.[115] Copyright 2018, SAGE Publications. c) The modulus of a Miura-ori sheet can also be reprogrammed via introducing pop-through defects (PTD), which are nonrigid folding, bistable deformations. Adapted with permission.[116] Copyright 2014, American Association for the Advancement of Sciences. d) A bistable kresling module used in the Flexigami materia. Adapted with permission.[117] Copyright 2018, Elsevier. Its force-displacement curves clearly show the two stable states.

Origami Materials Based on Rigid-Foldable Designs: By definition, this kind of origami can fold smoothly only by concentrated crease folding without inducing any facet deformations, so their total potential energy is a summation of the constituent crease energies (as we detailed in Section 3.1). Since the accessible configuration space of rigid-foldable origami is well defined, the landscape of elastic potential energy can be calculated directly according to the prescribed origami pattern, creases torsional stiffness, and their rest angles. Multiple energy

minima (aka multistability) can be obtained by exploiting the nonunique mapping between folding and crease opening angle, that is, crease deformation can be the same at different folding configurations. For example, the generic degree-4 vertices can be highly multistable with careful designs.[74] A numerical analysis based on a uniform sampling of its design space revealed that a generic degree-4 vertex can possess 2 to 5 stable states; while a doubly symmetric vertex possesses up to 6 stable states. These results suggest the possibility of constructing

shape-reconfigurable and multistable "meta-sheets" with powerful morphing capabilities (Figure 6a). Higher order vertices, such as the water bomb base[118] and leaf-out pattern[119] can also be multistable. For example, the leaf-out origami pattern, which includes a degree-8 vertex at its center, features different one-degree-of-freedom deployment "schemes" and the symmetric scheme turned out to be bistable.

Rigid-foldable origami materials consisting of stacked sheets and assembled modules can also be multistable. For example, the reentrant TMP shown in Figure 4b can be bistable with specific combinations of facet design and rest angle assignments.[66] This bistability, combined with aforementioned auxetic properties, has great potentials for impact absorption and large stroke actuation. The stacked Miura-ori can display multistability if the crease torsional stiffness of adjacent Miura-ori sheets are significantly different. One stable state occurs at the nested-in configuration and the other at bulged-out configuration. If fluidic pressure is supplied to the tubular channels, the stacked Miura-ori can be switched among being mono-stable, bistable, and multistable,[102] offering the capability of rapid and autonomous shape reconfiguration. Furthermore, the fundamentally 3D nature of folding can impart some unorthodox multistability properties that can be harnessed for elastic modulus programming[115] (Figure 6b) and even mechanical diode effect.[75] Other than the TMP and stacked Miura-ori, many other origami assembly, such as the lantern inspired Kirigami modules in Figure 1d,[63] have also been demonstrated to exhibit multistability based on similar physical principles.

Origami Materials Based on Nonrigid Foldable Designs: This kind of origami folds by a combination of facet deformation and crease bending, and the compliance of facet allows the origami to access the otherwise unavailable folding configurations. In this case, multistability can arise if the origami possesses multiple configurations where its facets are un-deformed, but the transition between these configurations requires significant facet buckling or bending. For example, one can create reversible and bistable pop-through defects (PTDs) in the classic Miura-ori sheet (Figure 6c).[116] This phenomenon emerges due to the presence of "accessible" bending modes as the facet bending stiffness becomes comparable to the crease folding stiffness. The PTDs can be used to program the compressive modulus of Miura-ori by strategically placing/removing defect pairs, leading to a new class of re-programmable metamaterial. In another example, kirigami cutting principles were applied to create a bioinspired, bistable origami cell with potential applications in shape morphing and camouflage.[120] An array of these cells was created by combining stiff ABS facets and flexible silicone facets which are pneumatically actuated. A sub-millimeter scale, polymer-gel based square twist pattern was also demonstrated to be bistable.[76] This nonrigid foldable pattern is always mono-stable if the ratio of facet bending over crease torsional stiffness is smaller than 1 (aka $K_f/K_c < 1$) and it is always bistable if this ratio exceeds 1000 ($K_f/K_c > 10^3$). Thus, the bistability in such origami patterns can be controlled by changing the facet to crease stiffness ratio. Kresling is another well-studied bistable and nonrigid foldable crease pattern, which has been studied for its potential applications in deployable structures[89] and robotic locomotion.[24] Recently, a Kresling derived pattern called Flexigami (Figure 6d), where slit cuts are

introduced to impart additional compliance, has been shown to exhibit superior specific modulus than the current low-density materials.[117] Thus, a stacked Flexigami has the potential to be used as multifunctional deployable cellular material.

4.4. Dynamics

The aforementioned studies mainly focused on static or quasi-static characteristics of the architected origami materials. However, their intricate nonlinear elastic properties could lead to interesting dynamic characteristics and applications. Nevertheless, studying the dynamics of folding is still a nascent field and there are only a few researches conducted in this area. One study by Yasuda et al. examined the nonlinear elastic wave propagation in a multiple degree-of-freedom origami material consisting of TMP modules.[121] They examined the formation of rarefaction waves due to the geometry-induced elastic nonlinearity of TMP modules, and explored the feasibility of using such nonlinear wave propagation for tunable vibration and impact mitigating. Another study investigated the base excitation response of the bistable stacked Miura-ori cell through both numerical simulation and experiments.[122] The results revealed that the intra and inter-well dynamics of the bistable stacked Miura-ori are strongly influenced by the asymmetry in its force-deformation relationship. A cylindrical truss structure inspired by the Kresling folding pattern were investigated for vibration isolation both numerically and experimentally.[123,124] This vibration isolation function stemmed from a quasi-zero stiffness (QZS) property obtained by integrating a linear spring with the bistable Kresling pattern. In an experimental demonstration, the Kresling vibration isolator managed to isolate 21% of the wave energy in the Tohoku–Pacific Ocean earthquake and 6% of the Kobe earthquake. The aforementioned fluidic origami can also generate quasi-zero stiffness properties for vibration isolation.[104] Unlike the Kresling-based cylindrical truss structure, the QZS properties of the fluidic origami did not arise from mechanical springs but rather originated from the interaction between internal pressure and folding. This provided a unique mechanism for developing an adaptive QZS vibration isolator. In another study, the nonlinear dynamics of an adaptive origami stent system was numerically simulated to understand its deployment.[125]

Besides the dynamics of reciprocal folding, the geometric periodicity in origami materials also makes them versatile acoustic metamaterials. In this case, folding offers a pathway to tailor the underlying periodicity to achieve tunable acoustic behaviors. For example, rigid-folding of Miura-ori sheet can arrange the attached inclusions into square, hexagonal, rectangular, and asymmetrical patterns, thus significantly tailor and frequency spectrum of the corresponding acoustic bandgaps.[126,127] Such and similar features have been utilized for noise mitigation,[126–128] wave guiding[129,130] and focusing.[131]

4.5. Impact Absorption

Numerical and experimental studies on the impact absorption performance of origami foldcore materials are extensive due to their potential applications in the aerospace structures.

An excellent paper by Heimbs reviewed the early studies in this topic,[78] so this section focuses on briefly discussing the essential physical principles and recent progresses. Due to the nonrigid foldable nature, the origami foldcore deforms in different ways based on the loading condition. Under quasi-static loading or low-velocity impact (that is, the impact velocity is lower than the elastic wave propagation speed), the foldcore consisting of conventional Miura-ori sheets typically fails via facet buckling or fracturing (**Figure 7**a).[78] Buckling occurs if the Miura-ori is made of ductile materials like the aramid fabrics, and fracture is more likely if the material is brittle like carbon reinforced composite. Nonetheless, both failure modes are capable of absorbing impact energy. Especially, if the impact is local, the zig-zag shaped origami creases can act like a stopper to localize damage.[78] To further improve the impact absorption performance, indented folds can be added to the Miura-ori sheets to induce a different failure mode called travelling hinge line (THL).[92,132] In this mode, the additional creases from indented folds can travel along the facet, creating a more uniform reaction stress (Figure 7b). Under high velocity impact from a solid projectile, the face skins absorb most of the impact energy through highly localized fracturing and

de-bonding between the skin and origami core. However, under blast impact (aka a nonuniform external pressure field), both face skin stretching and origami facet buckling play important roles.[133,134] Curved creases[91,94] and the Kirigami cutting[135,136] (Figure 7c) were explored to obtain superior impact absorption than Miura-ori and its derivatives, and their geometric designs can be tailored for performance optimization. It is found that the optimized origamis typically feature facets orientated near perpendicular to the face skins.[78] However, even based on the optimized origami core designs, experimental test results from the foldcore samples are consistently lower than the numerical predictions,[107,137,138] and the imperfection plays a crucial role in this discrepancy. Imperfection can originate from inaccurate origami geometry, nonuniform material property, as well as imperfect bonding between face skin and origami core. Therefore, various methods have been recently examined to incorporate these imperfection for better numerical accuracy.[95,139–141]

It is worth highlighting that besides the aforementioned mechanical properties, the architected origami materials have also shown protentials in reconfigurable electromagnetic[142,143] and thermo applications,[144] however, discussion on these topics are beyond the scope of this paper.
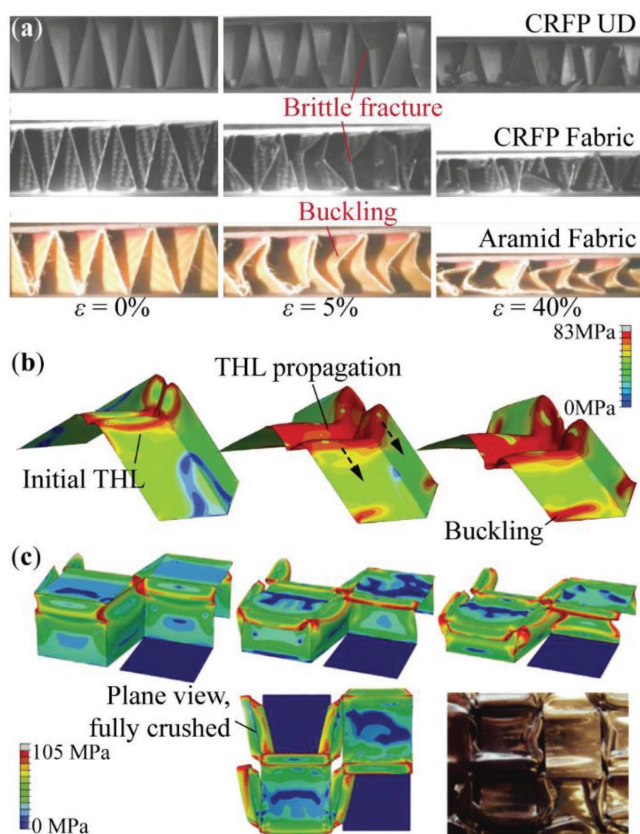
4.6. Potential Applications of the Folding Induced Properties

The long list of mechanical properties available from origami materials leads to many potential applications. For example, the auxetic properties are known to increase the shear and indentation resistance,[145] and provide strain amplification.[146] The shape re-configuration capabilities by folding have great potentials in shape morphing for high performance aircrafts and vehicles.[147,148] Studies on the nonlinear stiffness properties of origami can lay down the foundation for building relatively light, stiff, yet reconfigurable materials for adaptive civil infrastructures.[16] Many nonlinear stiffness properties of origami, like the discrete stiffness jumps and quasi-zero stiffness, can be used for low-frequency vibration isolation and absorption.[149] The multistability from folding is probably the most promising properties to impart multifunctionality in structures and material systems. In addition to the property programming and mechanical diode effect discussed in Section 4.3, multistability can also be exploited to achieve broadband vibration control,[150] energy harvesting,[151] and even robotic locomotion.[152,153] Studies on the impact absorption of foldcore materials have paved the way for commercial applications in aerospace and automotive industries.

5. A Highlight on Fabrication Techniques

Fabrication of the architected origami materials is essentially a process of creasing and manipulating thin sheets into desired 3D shapes, so that the aforementioned material properties can be realized for practical implementations. Fabrication of origami materials benefits greatly from the aforementioned developability characteristics, meaning that the complex shapes of origami can all be developed from folding a flat piece of sheet material. This is a procedure that can be automated so that origami materials can be made efficiently and rapidly. Here,

Figure 7. Impact absorption studies of different origami materials. a) Experimental results showing the facet failures in a Miura-ori based foldcore under low velocity impact. Adapted with permission.[78] Copyright 2013, Springer Nature. b) Traveling hinge line (THL) propagation in a indented Miura-ori core under quasi-static compressive load. Reproduced with permission.[132] Copyright 2014, Elsevier. c) Finite element simulation and experiment showing the facet crushing in the chess-board pattern shown in Figure 2b. Reproduced with permission.[135] Copyright 2015, Elsevier.

a successful fabrication technique should be able to create a periodic pattern of *both* mountain and valley creases at different size scales (typically, the length of a crease line is smaller than 1 cm). It should also be able to effectively assemble a large number of folded origami sheets or modules together when necessary. It is worth noting that there is a large number of literatures on advanced fabrication via folding, and interested readers can refer to the reviews by Shenoy and Gracias,[30] Xin Ning et al.,[42] and Yihui et al.[154] for more information. The following subsections briefly highlight two fabrication strategies that have been shown capable of producing the desired periodic tessellation of both mountain and valley creases.

5.1. By External Mechanical Force

Using external force to crease and fold origami sheets is effective and applicable for a wide variety of material selections such as paper, plastic, and metal sheets, etc. Folding by hand obviously is the most intuitive example, and it is still arguably the most powerful way to fold paper into extremely complicated shapes.[57,61,155,156] Indeed, hand folded paper Miura-ori can be carbonized directly into a structural material for load bearing and electro-chemical applications (**Figure 8**a).[157] Customized press machines were also used to successfully fabricate fold-core material in large quantities.[78] Before folding, the raw sheet materials are usually creased according to the desired pattern by plotter cutter, laser cutter, or chemical etching.

Folding by hand or press machine, however, can only create relatively large origami sheets where the crease lines are at least centimeter long. *Buckling induced folding* is a very promising method to address this shortcoming. The physical principle underlying this buckling based method is simple and scalable: Thin sheets subjected to in-plane compressive stress can buckle out-of-plane and generate 3D geometric features.[44,158,159] If the thin sheet has embedded origami creasing,
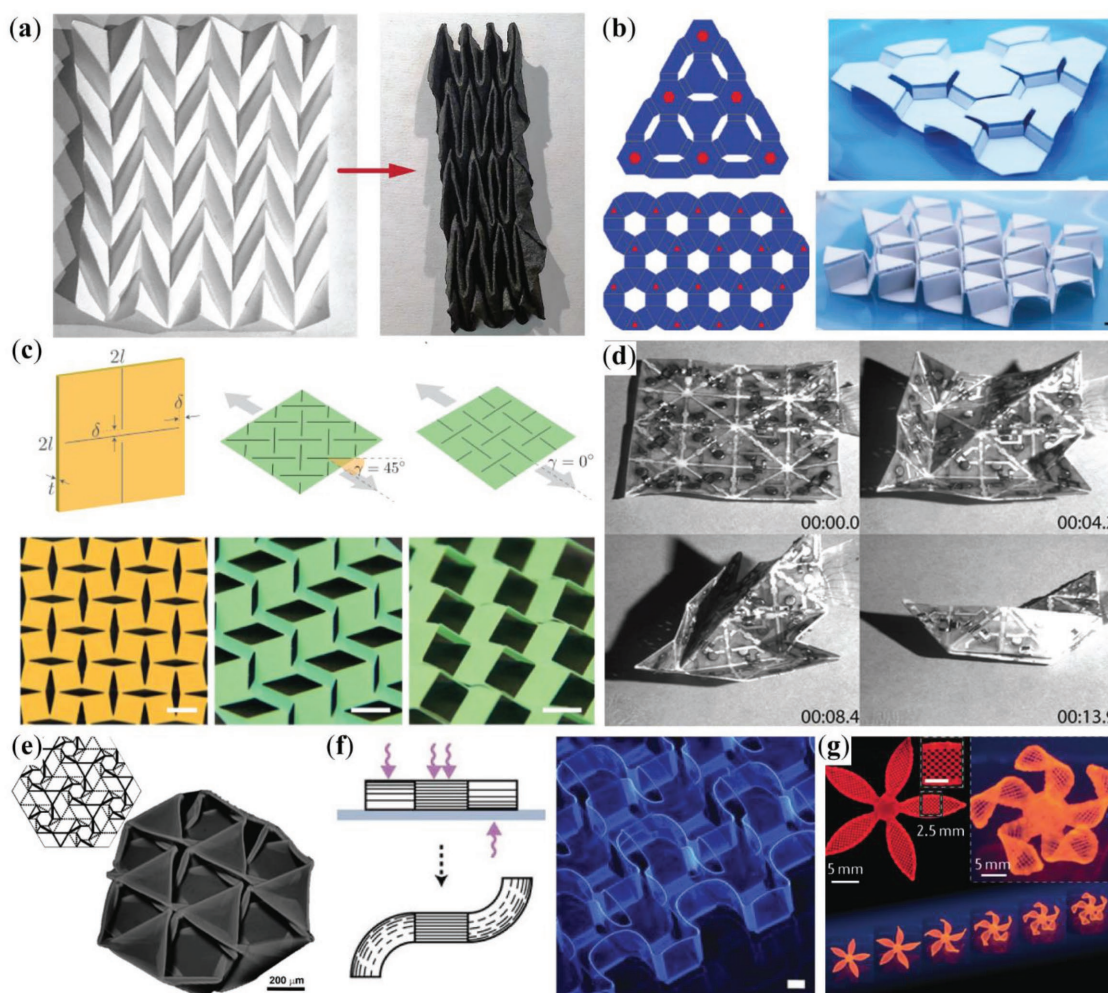

Figure 8. Examples of fabrication techniques that can produce bidirectional, periodic, and small scale folds, which are essential for constructing architected origami materials. a) Carbon origami based on hand folded Miura-ori paper. Reproduced with permission.[157] Copyright 2018, Elsevier. b) Mechanically guided, compressive buckling induced folding. Reproduced with permission.[48] Copyright 2016, Wiley-VCH. c) Stretching induced buckling. Reproduced with permission.[161] Copyright 2017. d) Self-folding induced by embedded shape memory alloy (SMA). Reproduced with permission.[162] Copyright 2015, National Academy of Sciences. e,f) Cross-linking layers of passive and active polymers. e) Reproduced with permission.[163] Copyright 2015, Wiley-VCH. f) Reproduced with permission.[164] Copyright 2011, Springer Nature. g) 4D printing. Reproduced with permission.[165] Copyright 2016, Springer Nature.

the buckling induced deformation can concentrate along these crease lines and effectively create coordinated folding. A mechanically guided folding technique was recently developed by exploiting this principle (Figure 8b).[47,48,160] First, thin films (or 2D precursors) with nonuniform thickness and slit cuts are fabricated by 2D fabrication methods (e.g., photolithography and etching). The finished precursors were then attached to a pre-stretched silicone elastomer substrate at designated "bonding sites." Chemical treatments were applied at these bonding sites to ensure a strong adhesion between precursor and silicone substrate, and sacrificial layers were added underneath nonbonding regions (aka facets and creases) to eliminate the undesired adhesion from van der Waals forces. Finally, the pre-stretch in the silicone substrate was released to create the compressive stress needed to buckle and fold the origami sheet. This method can produce complex and periodic origami/kirigami features at vastly different length scales (from micrometer to meter), therefore, it is a promising method for fabricating the architected origami materials. Besides compressive stress, extension stress applied to a 2D Kirigami sheet with purposefully distributed slits cuts can also generate buckling deformation and eventually folding (Figure 8c).[161]

5.2. By Internal Stress Mismatch (Self-Folding)

The idea of self-folding is to make the crease lines "active," so that they can fold by themselves with external stimuli other than the mechanical force (e.g., heat, humidity, light, etc.). Such autonomous folding requires internal bending moments along the crease lines, and they can be generated by inducing a nonuniform stress distribution through the thickness. That is, if the internal stress at the bottom half of the crease line region is higher than the upper half, a valley fold will be created; on the other hand, a mountain fold is created when the internal stress is higher at the upper half. The neutral plane of such folding deformation is directly related to the sheet material thickness, stiffness, and internal stress distribution, so careful designs are necessary to ensure that the neutral plane is well positioned to induce effective folding. This is especially important if any electronic components are embedded in the origami sheet.[166] A wide variety of response materials, such as shape memory alloys and hydrogels, are well-suited for generating the required internal stress mismatch and some of them can be fabricated at micro- and even nanoscale. However, current state of the art are mostly limited to creating simple geometries such as polyhedrons, tubes, and curved surfaces. Only a few techniques have demonstrated the capability of producing a periodic arrangement of both mountain and valley folds that are essential for constructing architected materials. Here we provide a brief highlight of these approaches.

Bimorph and Trimorph Crease: This is a well-studied method to create active crease lines for self-folding. The idea is to embed two or three layers of *different* responsive materials along the designated crease lines, so that they can generate the desired internal stress mismatch in response to the external stimuli. A bimorph design can provide unidirectional bending, while the trimorph can provide bidirectional folding for both mountain and valley folds. Moreover, if the stress can be relieved by removing the stimuli, the self-folding becomes reversible.

Embedding a layer of shape memory alloy (SMA) into a thin polymer sheet is a common method to achieve self-folding at the millimeter scale (Figure 8d),[167] this method has shown superior controllability and programmability by simple electric current inputs.[162,168] Bimorph and trimorph active creases were also fabricated at smaller scales by applying a layer of molten solder on Au films,[169] lithographically patterning chromium and copper layers[51] (Figure 1c), and crosslinking layers of passive and active polymers[163] (Figure 8e).

Differential Swelling in Monolithic Material: A layer of monolithic responsive material can exhibit self-folding if the magnitude of stress generation varies through its thickness. For example, by carefully controlling the ultraviolet exposure energy and direction, a photodefinable epoxy film (SU-8) can be made with a gradient of cross-linking, which creates a differential swelling for controlled bending and folding (Figure 8f).[164] Similar mechanism was also achieved in liquid crystal elastomer sheet by controlling the direction of the molecular order through the film thickness.[170] Achieving such differential swellings typically requires a very intricate control of the fabrication process, and the material selections are relatively limited. This technique has more potentials for creating soft origami materials capable of reversible folding.

4D Printing: An increasingly popular method of achieving self-folding is 4D printing, where the fourth dimension refers to time. By this method, 3D printing techniques forms a heterogeneous sheet with layers of passive and active materials (such as shape memory polymer[171,172] or hydrogel[165,173]), and desired origami shape can be achieved by applying appropriate stimuli after printing (Figure 8g). 4D printing is a variation of the bimorph and trimorph method, and the general accessibility of the 3D printers makes it a promising technique for constructing the architected origami materials.

It is worth noting that besides using the responsive materials, many other techniques have been established to achieve self-folding at different length scales, such as using surface tension,[112,174] thermal expansion,[175] intrinsic residual stress in thin film,[176,177] and lattice mismatch.[178] Although the folding pattern generated by these techniques are relatively simple at this stage, further development will surely enrich the origami material fabrication especially at smaller sizes.

6. Discussion, Challenges, and Future Directions

This report details the recent progress of architected origami materials regarding their geometric design strategies, mechanics models, achieved properties and relevant fabrication techniques. The intricate geometry and kinematics of folding offers the possibility to achieve many desirable and even unorthodox material properties, such as auxetics, on-demand tunable stiffness, multistability, vibration and impact management. The developability and scalability of folding offers the possibility to fabricate origami materials at vastly different sizes without losing the desired properties. Moreover, development of origami materials is also causing the theories of origami mechanics to evolve, which reveals how the constitutive properties and spatial orientations of facets and creases can be designed for the targeted material properties. Finally, the topic

of origami materials is facilitating the synergy between different branches of origami research—including crease design, analytical modeling, and fabrication—which had been individually and separately evolving.

On the other hand, there are several challenges need to be addressed in order to enable this exciting opportunity to mature and flourish. The first challenge is on origami design. Currently the most popular strategy in designing origami materials is to directly use the available folding patterns, like the classic Miura-ori, even though they were created for other purposes. This approach has led to interesting results so far, however, it does not fully leverage the vast design space in origami. Different crease design methods are available, like the popular "tree method,"[6] but they are intended for achieving a desired shape by folding rather than a specific material property. Therefore, an important next step in this field is to derive an origami crease design methodology that can incorporate the mechanics of folding. This new methodology will combine the geometric constraints for proper folding, such as developability and periodicity, and the different mechanics model of origami. It should be able to search and create crease folding pattern with computational efficiency.

The second challenge is on mechanics modeling. Although quite a few origami mechanics model are available (as detailed in Section 3), none of them has the desired combination of high computational efficiency and analytical accuracy. The different types of truss-frame models are capable of qualitatively analyzing the mechanics of origami, however, none of them so far have shown any quantitative agreements with *experimental* results, which were typically obtained on universal testing machines. Such discrepancies can be significant when large facet deformations are observed like in the nonrigid-foldable origamis. Finite element simulation, on the other hand, is quite computationally expensive partly because there's no elements specifically tailored for origami problems. Moreover, experimental results from the origami material prototypes show significant variations due to the unknown and uncertain parameters, this might require some identification methods to be incorporated into origami mechanics model.[179] Indeed, the lack of an accurate and computationally efficient model could be a critical issue for this field, so much efforts are needed to advance the state of the art.

The next challenge is the further study into the dynamic characteristic of folding. So far the vast majority of origami related research focuses on static or quasi-static behaviors, however, the few studies discussed in this report suggested that the dynamic behaviors of origami materials have strong potentials for many applications like low-frequency base excitation isolation and wave propagation control. Understanding the dynamic characteristics induced by reciprocal folding is still a relatively open research topic.

Research on the fabrication of architected materials via origami folding faces its own unique challenges. For example, the ideal self-folding mechanism should be able to induce, orient, and pattern highly localized stresses in a variety of thin film materials with minimal manual interventions. It is still difficult to develop such self-folding schemes that can satisfy all of these requirements. The buckling induced folding mechanism requires new design rules for mapping the desired folded shape onto the thin film precursors.

Challenges related to the synergy between different branches of origami research are still pressing. A successful development of origami materials for practical applications will need tighter integration of design, mechanics analysis, and fabrication, because they can impose constraints on each other. For example, the fabrication of origami materials, especially at smaller scale, requires careful considerations of the finite sheet thickness and fabrication uncertainties. But almost all of the currently available origami mechanics models assume zero sheet thickness or perfect geometry. On the other hand, many origami material designs are based on the strategies of stacking sheets or assembling modules, however, none of the aforementioned fabrication techniques can achieve these outcomes, except for 3D printing. Gaps between the different aspects of developing architected origami materials need to be examined and bridged.

Finally, while many interesting mechanical properties have been achieved in the origami materials, we haven't seen many concrete applications of these properties in real products. The current state of the art focuses on revealing the potentials of origami materials and its applications, however, identifying real-world applications in which origami materials can outperform other technologies is crucial for the long term sustainability of this research topic.

Conflict of Interest

The authors declare no conflict of interest.

[1] M. McArthur, R. J. Lang, *Folding Paper: The Infinite Possibilities of Origami*, Tuttle Publishing, Rutland, VT, USA **2013**.

[2] T. C. Hull, *Project Origami: Activities for Exploring Mathematics*, CRC Press, Boca Raton, FL, USA **2012**.

[3] M. Fiol, N. Dasquens, M. Prat, in *Origami 5*, (Eds: P. Wang-Iverson, R. J. Lang, M. Yim), A K Peters/CRC Press, Boca Raton, FL, USA **2011**, pp. 151–164.

[4] J. Kennedy, E. Lee, A. Fontecchio, in *IEEE Front. Educ. Conf.*, IEEE, Piscataway, NJ, USA **2016**.

[5] N. J. Boakes, in *Origami 5*, (Eds: P. Wang-Iverson, R. J. Lang, M. Yim), A K Peters/CRC Press, Boca Raton, FL, USA **2011**, pp. 173–187.

**ADVANCED
SCIENCE NEWS**
www.advancedsciencenews.com

**ADVANCED
MATERIALS**
www.advmat.de

[6] R. J. Lang, in *ACM Symp. on Computational Geometry*, ACM Press, New York, NY, USA **1996**, pp. 98–105.

[7] E. D. Demaine, J. O'Rourke, *Geometric Folding Algorithms: Linkages, Origami, Polyhedra*, Cambridge University Press, New York, NY, USA **2007**.

[8] E. R. Adrover, *Deployable Structures*, Laurence King, London, UK **2015**.

[9] M. Buchanan, *Nat. Phys.* **2017**, *13*, 318.

[10] D. Dureisseix, *Int. J. Space Struct.* **2012**, *27*, 1.

[11] E. A. Peraza-Hernandez, D. J. Hartl, R. J. Malak Jr., D. C. Lagoudas, *Smart Mater. Struct.* **2014**, *23*, 094001.

[12] A. Lebée, *Int. J. Space Struct.* **2015**, *30*, 55.

[13] M. Schenk, A. D. Viquerat, K. A. Seffen, S. D. Guest, *J. Spacecr. Rockets* **2014**, *51*, 762.

[14] S. A. Zirbel, R. J. Lang, M. W. Thomson, D. A. Sigel, P. E. Walkemeyer, B. P. Trease, S. P. Magleby, L. L. Howell, *J. Mech. Des.* **2013**, *135*, 111005.

[15] T. Tachi, in *Origami 5* (Eds: P. Wang-Iverson, R. J. Lang, M. Yim), A K Peters/CRC Press, Boca Raton, FL, USA **2011**, pp. 253–264.

[16] E. T. Filipov, T. Tachi, G. H. Paulino, *Proc. Natl. Acad. Sci. USA* **2015**, *112*, 12321.

[17] Y. Chen, R. Peng, Z. You, *Science* **2015**, *349*, 396.

[18] S. Felton, M. Tolley, E. D. Demaine, D. Rus, R. Wood, *Science* **2014**, *345*, 644.

[19] S. Miyashita, S. Guitron, M. Ludersdorfer, C. R. Sung, D. Rus, in *2015 IEEE Int. Conf. Robot. Autom.*, IEEE, Piscataway, NJ, USA **2015**, pp. 1490–1496.

[20] A. Firouzeh, J. Paik, *J. Mech. Rob.* **2015**, *7*, 021009.

[21] E. Vander Hoff, Donghwa J., Kiju L., in *2014 IEEE/RSJ Int. Conf. Intell. Robot. Syst.*, IEEE, Piscataway, NJ, USA **2014**, pp. 1421–1426.

[22] S. Miyashita, S. Guitron, K. Yoshida, Shuguang L., D. D. Damian, D. Rus, in *2016 IEEE Int. Conf. Robot. Autom.*, IEEE, Piscataway, NJ, USA **2016**, pp. 909–916.

[23] S. Miyashita, S. Guitron, S. Li, D. Rus, *Sci. Rob.* **2017**, *2*, eaao4369.

[24] A. Pagano, T. Yan, B. Chien, A. Wissa, S. Tawfick, *Smart Mater. Struct.* **2017**, *26*, 094007.

[25] H. Fang, Y. Zhang, K. W. Wang, *Bioinspiration Biomimetics* **2017**, *12*, 065003.

[26] C. L. Randall, E. Gultepe, D. H. Gracias, *Trends Biotechnol.* **2012**, *30*, 138.

[27] M. Johnson, Y. Chen, S. Hovet, S. Xu, B. Wood, H. Ren, J. Tokuda, Z. T. H. Tse, *Int. J. Comput. Assist. Radiol. Surg.* **2017**, https://doi.org/10.1007/s11548-017-1545-1.

[28] L. Xu, T. C. Shyu, N. A. Kotov, *ACS Nano* **2017**, *11*, 7587.

[29] F. Cavallo, M. G. Lagally, *Nano Today* **2015**, *10*, 538.

[30] V. B. Shenoy, D. H. Gracias, *MRS Bull.* **2012**, *37*, 847.

[31] P. Wang, T. A. Meyer, V. Pan, P. K. Dutta, Y. Ke, *Chem* **2017**, *2*, 359.

[32] M. Schenk, S. D. Guest, *Proc. Natl. Acad. Sci. USA* **2013**, *110*, 3276.

[33] Z. Y. Wei, Z. V Guo, L. H. Dudte, H. Y. Liang, L. Mahadevan, *Phys. Rev. Lett.* **2013**, *110*, 215501.

[34] C. Lv, D. Krishnaraju, G. Konjevod, H. Yu, H. Jiang, *Sci. Rep.* **2015**, *4*, 5979.

[35] N. A. Fleck, V. S. Deshpande, M. F. Ashby, *Proc. R. Soc. A* **2010**, *466*, 2495.

[36] J. H. Lee, J. P. Singer, E. L. Thomas, *Adv. Mater.* **2012**, *24*, 4782.

[37] A. A. Zadpoor, *Mater. Horiz.* **2016**, *3*, 371.

[38] J. Bauer, L. R. Meza, T. A. Schaedler, R. Schwaiger, X. Zheng, L. Valdevit, *Adv. Mater.* **2017**, *29*, 1701850.

[39] K. Bertoldi, V. Vitelli, J. Christensen, M. van Hecke, *Nat. Rev. Mater.* **2017**, *2*, 17066.

[40] N. Turner, B. Goodwine, M. Sen, *Proc. Inst. Mech. Eng., Part C* **2015**, *230*, 2345.

[41] S. J. P. Callens, A. A. Zadpoor, *Mater. Today* **2018**, *21*, 241.

[42] X. Ning, X. Wang, Y. Zhang, X. Yu, D. Choi, N. Zheng, D. S. Kim, Y. Huang, Y. Zhang, J. A. Rogers, *Adv. Mater. Interfaces5*, **2018**, 1800284.

[43] D. Rus, M. T. Tolley, *Nat. Rev. Mater.* **2018**, *3*, 101.

[44] S. Xu, Z. Yan, K. I. Jang, W. Huang, H. Fu, J. Kim, Z. Wei, M. Flavin, J. McCracken, R. Wang, A. Badea, Y. Liu, D. Xiao, G. Zhou, J. Lee, H. U. Chung, H. Cheng, W. Ren, A. Banks, X. Li, U. Paik, R. G. Nuzzo, Y. Huang, Y. Zhang, J. A. Rogers, *Science* **2015**, *347*, 154.

[45] C. M. Wheeler, M. L. Culpepper, *J. Mech. Rob.* **2016**, *8*, 051012.

[46] R. V Martinez, C. R. Fish, X. Chen, G. M. Whitesides, *Adv. Funct. Mater.* **2012**, *22*, 1376.

[47] Y. Zhang, Z. Yan, K. Nan, D. Xiao, Y. Liu, H. Luan, H. Fu, X. Wang, Q. Yang, J. Wang, W. Ren, H. Si, F. Liu, L. Yang, H. Li, J. Wang, X. Guo, H. Luo, L. Wang, Y. Huang, J. A. Rogers, *Proc. Natl. Acad. Sci. USA* **2015**, *112*, 11757.

[48] Z. Yan, F. Zhang, J. Wang, F. Liu, X. Guo, K. Nan, Q. Lin, M. Gao, D. Xiao, Y. Shi, Y. Qiu, H. Luan, J. H. Kim, Y. Wang, H. Luo, M. Han, Y. Huang, Y. Zhang, J. A. Rogers, *Adv. Funct. Mater.* **2016**, *26*, 2629.

[49] S. Tibbits, *Active Matter*, The MIT Press, Cambridge, MA, USA **2017**.

[50] J. T. B. Overvelde, J. C. Weaver, C. Hoberman, K. Bertoldi, *Nature* **2017**, *541*, 347.

[51] N. Bassik, G. M. Stern, D. H. Gracias, *Appl. Phys. Lett.* **2009**, *95*, 091901.

[52] D. Huffman, *IEEE Trans. Comput.* **1976**, *C-25*, 1010.

[53] T. Tachi, in *Int. Assoc. Shell Spat. Struct. Symp.*, Valencia, Spain **2009**, pp. 2287–2294.

[54] D. Fuchs, S. Tabachnikov, *Am. Math. Mon.* **1999**, *106*, 27.

[55] K. Miura, *ISAS Rep.* **1972**, *37*, 137.

[56] Y. Chen, H. Feng, J. Ma, R. Peng, Z. You, *Proc. R. Soc. A* **2016**, *472*, 20150846.

[57] T. Nojima, K. Saito, *JSME Int. J. Ser. A* **2006**, *49*, 38.

[58] T. Castle, Y. Cho, X. Gong, E. Jung, D. M. Sussman, S. Yang, R. D. Kamien, *Phys. Rev. Lett.* **2014**, *113*, 245502.

[59] Y. Hou, R. Neville, F. Scarpa, C. Remillat, B. Gu, M. Ruzzene, *Composites, Part B* **2014**, *59*, 33.

[60] T. Tachi, *J. Mech. Des.* **2013**, *135*, 111006.

[61] I. Stewart, *Nature* **2007**, *448*, 419.

[62] H. Fang, S. Li, H. Ji, K. W. Wang, *Phys. Rev. E* **2016**, *94*, 043002.

[63] N. Yang, J. L. Silverberg, *Proc. Natl. Acad. Sci. USA* **2017**, *114*, 3590.

[64] H. Yasuda, T. Yein, T. Tachi, K. Miura, M. Taya, *Proc. R. Soc. A* **2013**, *469*, 20130351.

[65] E. T. Filipov, G. H. Paulino, T. Tachi, *Proc. R. Soc. A* **2016**, *472*, 20150607.

[66] H. Yasuda, J. Yang, *Phys. Rev. Lett.* **2015**, *114*, 185502.

[67] S. Kamrava, D. Mousanezhad, H. Ebrahimi, R. Ghosh, A. Vaziri, *Sci. Rep.* **2017**, *7*, 46046.

[68] J. T. B. Overvelde, T. A. de Jong, Y. Shevchenko, S. A. Becerra, G. M. Whitesides, J. C. Weaver, C. Hoberman, K. Bertoldi, *Nat. Commun.* **2016**, *7*, 10929.

[69] T. Tachi, in *Adv. Archit. Geom.* (Eds: C. Ceccato, L. Hesselgren, M. Pauly, H. Pottmann, J. Wallner), Springer Vienna, Vienna, Austria **2010**, pp. 87–102.

[70] S. Waitukaitis, M. van Hecke, *Phys. Rev. E* **2016**, *93*, 023003.

[71] L. H. Dudte, E. Vouga, T. Tachi, L. Mahadevan, *Nat. Mater.* **2016**, *15*, 583.

[72] X. Zhou, S. Zang, Z. You, *Proc. R. Soc. A* **2016**, *472*, 20160361.

[73] V. Brunck, F. Lechenault, A. Reid, M. Adda-Bedia, *Phys. Rev. E* **2016**, *93*, 033005.

[74] S. Waitukaitis, R. Menaut, B. G. Chen, M. van Hecke, *Phys. Rev. Lett.* **2015**, *114*, 055503.

[75] H. Fang, K. W. Wang, S. Li, *Extreme Mech. Lett.* **2017**, *17*, 7.

[76] J. L. Silverberg, J. H. Na, A. A. Evans, B. Liu, T. C. Hull, C. D. Santangelo, R. J. Lang, R. C. Hayward, I. Cohen, *Nat. Mater.* **2015**, *14*, 389.

[77] B. Liu, A. A. Evans, J. L. Silverberg, C. D. Santangelo, R. J. Lang, T. C. Hull, I. Cohen, *arXiv:1706.01687* **2017**.

**ADVANCED
SCIENCE NEWS**

www.advancedsciencenews.com

**ADVANCED
MATERIALS**

www.advmat.de

[78] S. Heimbs, in *Dynamic Failure of Composite and Sandwich Structures* (Eds: S. Abrate, B. Castanié, Y. D. S. Rajapakse), Springer Netherlands, Dordrecht, The Netherlands **2013**, pp. 491–544.

[79] M. Schenk, S. D. Guest, in *Origami 5* (Eds: P. Wang-Iverson, R. J. Lang, M. Yim), A K Peters/CRC Press, Boca Raton, FL **2011**, pp. 291–304.

[80] A. A. Evans, J. L. Silverberg, C. D. Santangelo, *Phys. Rev. E* **2015**, *92*, 013205.

[81] T. A. Witten, *Rev. Mod. Phys.* **2007**, *79*, 643.

[82] K. Fuchi, P. R. Buskohl, G. Bazzan, M. F. Durstock, G. W. Reich, R. A. Vaia, J. J. Joo, *J. Mech. Des.* **2015**, *137*, 091401.

[83] S. Li, K. W. Wang, *Smart Mater. Struct.* **2015**, *24*, 105031.

[84] S. D. Guest, *Int. J. Solids Struct.* **2006**, *43*, 842.

[85] E. T. Filipov, K. Liu, T. Tachi, M. Schenk, G. H. Paulino, *Int. J. Solids Struct.* **2017**, *124*, 26.

[86] K. Fuchi, P. R. Buskohl, J. J. Joo, G. W. Reich, R. A. Vaia, in *Origami 6*, American Mathematical Society, Providence, RI, USA **2015**, pp. 1–11.

[87] K. Liu, G. H. Paulino, *Proc. R. Soc. A* **2017**, *473*, 20170348.

[88] A. Gillman, K. Fuchi, P. R. Buskohl, *Int. J. Solids Struct.* **2018**, *147*, 80.

[89] J. Cai, X. Deng, Z. Ya, F. Jiang, Y. Tu, *J. Mech. Des.* **2015**, *137*, 061406.

[90] S. Fischer, K. Drechsler, S. Kilchert, A. Johnson, *Composites, Part A* **2009**, *40*, 1941.

[91] X. Zhou, H. Wang, Z. You, *Thin-Walled Struct.* **2014**, *82*, 296.

[92] J. Ma, Z. You, *J. Appl. Mech.* **2013**, *81*, 011003.

[93] S. Liu, G. Lu, Y. Chen, Y. W. Leong, *Int. J. Mech. Sci.* **2015**, *99*, 130.

[94] J. M. Gattas, Z. You, *Int. J. Solids Struct.* **2015**, *53*, 80.

[95] S. Fischer, *Int. J. Mech. Mater. Eng.* **2015**, *10*, 14.

[96] T. Smit, *Master's thesis*, Delft University of Technology, Delft, The Netherlands **2017**.

[97] R. Sturm, P. Schatrow, Y. Klett, *Appl. Compos. Mater.* **2015**, *22*, 857.

[98] A. Lebée, K. Sab, *Int. J. Solids Struct.* **2010**, *47*, 2620.

[99] A. Lebée, K. Sab, *Int. J. Solids Struct.* **2012**, *49*, 2778.

[100] M. Eidini, G. H. Paulino, *Sci. Adv.* **2015**, *1*, e1500224.

[101] W. Jiang, H. Ma, M. Feng, L. Yan, J. Wang, J. Wang, S. Qu, *J. Phys. D: Appl. Phys.* **2016**, *49*, 315302.

[102] S. Li, K. W. Wang, *J. R. Soc., Interface* **2015**, *12*, 20150639.

[103] S. Li, H. Fang, K. W. Wang, *Phys. Rev. Lett.* **2016**, *117*, 114301.

[104] S. Sadeghi, S. Li, in *Proc. ASME SMASIS*, ASME, Snowbird, UT, USA **2017**, pp. 2017–3754.

[105] H. Fang, S. A. Chu, Y. Xia, K. Wang, *Adv. Mater.* *30*, **2018**, 1706311.

[106] J. B. Berger, H. N. G. Wadley, R. M. McMeeking, *Nature* **2017**, *543*, 533.

[107] M. Kintscher, L. Kärger, A. Wetzel, D. Hartung, *Composites, Part A* **2007**, *38*, 1288.

[108] K. C. Cheung, T. Tachi, S. Calisch, K. Miura, *Smart Mater. Struct.* **2014**, *23*, 094012.

[109] J. M. Gattas, Z. You, *Eng. Struct.* **2015**, *94*, 149.

[110] D. Deng, Y. Chen, *J. Mech. Des.* **2015**, *137*, 021701.

[111] S. M. Felton, M. T. Tolley, B. Shin, C. D. Onal, E. D. Demaine, D. Rus, R. J. Wood, *Soft Matter* **2013**, *9*, 7688.

[112] T. G. Leong, P. A. Lester, T. L. Koh, Call EK, D. H. Gracias, E. K. Call, D. H. Gradias, *Langmuir* **2007**, *23*, 8747.

[113] H. Fang, S. Li, K. W. Wang, *Proc. R. Soc. A* **2016**, *472*, 20160682.

[114] J. Ma, J. Song, Y. Chen, *Int. J. Mech. Sci.* **2018**, *136*, 134.

[115] S. Sengupta, S. Li, *J. Intell. Mater. Syst. Struct.* **2018**, *29*, 2933.

[116] J. L. Silverberg, A. A. Evans, L. McLeod, R. C. Hayward, T. C. Hull, C. D. Santangelo, I. Cohen, *Science* **2014**, *345*, 647.

[117] N. Nayakanti, S. H. Tawfick, J. A. Hart, *Extreme Mech. Lett.* **2018**, *21*, 17.

[118] B. H. Hanna, J. M. Lund, R. J. Lang, S. P. Magleby, L. L. Howell, *Smart Mater. Struct.* **2014**, *23*, 094009.

[119] H. Yasuda, Z. Chen, J. Yang, *J. Mech. Rob.* **2016**, *8*, 031013.

[120] S. Daynes, R. S. Trask, P. M. Weaver, *Smart Mater. Struct.* **2014**, *23*, 125011.

[121] H. Yasuda, C. Chong, E. G. Charalampidis, P. G. Kevrekidis, J. Yang, *Phys. Rev. E* **2016**, *93*, 043004.

[122] H. Fang, S. Li, H. Ji, K. W. Wang, *Phys. Rev. E* **2017**, *95*, 052211.

[123] S. Ishida, H. Uchida, H. Shimosaka, I. Hagiwara, *J. Vib. Acoust.* **2017**, *139*, 031015.

[124] S. Ishida, K. Suzuki, H. Shimosaka, *J. Vib. Acoust.* **2017**, *139*, 051004.

[125] G. V. Rodrigues, L. M. Fonseca, M. A. Savi, A. Paiva, *Int. J. Mech. Sci.* **2017**, *133*, 303.

[126] M. Thota, S. Li, K. W. Wang, *Phys. Rev. B* **2017**, *95*, 064307.

[127] M. Thota, K. W. Wang, *J. Appl. Phys.* **2017**, *122*, 154901.

[128] P. P. Pratapa, P. Suryanarayana, G. H. Paulino, *J. Mech. Phys. Solids* **2018**, *118*, 115.

[129] S. Babaee, J. T. B. Overvelde, E. R. Chen, V. Tournat, K. Bertoldi, *Sci. Adv.* **2016**, *2*, e1601019.

[130] M. Thota, K. W. Wang, *J. Sound Vib.* **2018**, *430*, 93.

[131] R. L. Harne, D. T. Lynd, *Smart Mater. Struct.* **2016**, *25*, 085031.

[132] J. M. Gattas, Z. You, *Int. J. Impact Eng.* **2014**, *73*, 15.

[133] A. Pydah, R. C. Batra, *Thin-Walled Struct.* **2017**, *115*, 311.

[134] A. Pydah, R. C. Batra, *Thin-Walled Struct.* **2018**, *129*, 45.

[135] R. K. Fathers, J. M. Gattas, Z. You, *Int. J. Mech. Sci.* **2015**, *101–102*, 421.

[136] W. Chen, H. Hao, *Int. J. Impact Eng.* **2018**, *115*, 94.

[137] S. Heimbs, P. Middendorf, S. Kilchert, A. F. Johnson, M. Maier, *Appl. Compos. Mater.* **2007**, *14*, 363.

[138] S. Heimbs, J. Cichosz, M. Klaus, S. Kilchert, A. F. Johnson, *Compos. Struct.* **2010**, *92*, 1485.

[139] E. Baranger, P. A. Guidault, C. Cluzel, *Compos. Struct.* **2011**, *93*, 2504.

[140] S. Kilchert, A. F. Johnson, H. Voggenreiter, *Composites, Part A* **2014**, *57*, 16.

[141] R. Sturm, S. Fischer, *Appl. Compos. Mater.* **2015**, *22*, 791.

[142] K. Fuchi, T. Junyan, B. Crowgey, A. R. Diaz, E. J. Rothwell, R. O. Ouedraogo, *IEEE Antennas Wireless Propag. Lett.* **2012**, *11*, 473.

[143] Z. Wang, L. Jing, K. Yao, Y. Yang, B. Zheng, C. M. Soukoulis, H. Chen, Y. Liu, *Adv. Mater.* **2017**, *29*, 1700412.

[144] E. Boatti, N. Vasios, K. Bertoldi, *Adv. Mater.* **2017**, *29*, 1700360.

[145] K. E. Evans, A. Alderson, *Adv. Mater.* **2000**, *12*, 617.

[146] R. H. Baughman, *Nature* **2003**, *425*, 667.

[147] J. Sun, Q. Guan, Y. Liu, J. Leng, *J. Intell. Mater. Syst. Struct.* **2016**, *27*, 2289.

[148] S. Daynes, P. M. Weaver, *Proc. Inst. Mech. Eng., Part D* **2013**, *227*, 1603.

[149] R. A. Ibrahim, *J. Sound Vib.* **2008**, *314*, 371.

[150] R. L. Harne, K. W. Wang, *Harnessing Bistable Structural Dynamics: For Vibration Control, Energy Harvesting and Sensing*, John Wiley and Sons, Chichester, UK **2017**.

[151] S. P. Pellegrini, N. Tolou, M. Schenk, J. L. Herder, *J. Intell. Mater. Syst. Struct.* **2013**, *24*, 1303.

[152] T. Chen, O. R. Bilal, K. Shea, C. Daraio, *Proc. Natl. Acad. Sci. USA* **2018**, *115*, 5698.

[153] B. Treml, A. Gillman, P. Buskohl, R. Vaia, *Proc. Natl. Acad. Sci. USA* **2018**, 201805122.

[154] Y. Zhang, F. Zhang, Z. Yan, Q. Ma, X. Li, Y. Huang, J. A. Rogers, *Nat. Rev. Mater.* **2017**, *2*, 17019.

[155] B. Y. Ahn, D. Shoji, C. J. Hansen, E. Hong, D. C. Dunand, J. A. Lewis, *Adv. Mater.* **2010**, *22*, 2251.

[156] S. T. Brittain, O. J. A. Schueller, H. Wu, S. Whitesides, G. M. Whitesides, *J. Phys. Chem. B* **2001**, *105*, 347.

[157] M. Islam, J. Flach, R. Martinez-duarte, *Carbon* **2018**, *133*, 140.

[158] G. M. Whitesides, N. Bowden, S. Brittain, A. G. Evans, J. W. Hutchinson, *Nature* **1998**, *393*, 146.

[159] W. T. S. Huck, N. Bowden, P. Onck, T. Pardoen, J. W. Hutchinson, G. M. Whitesides, *Langmuir* **2000**, *16*, 3497.

**ADVANCED
SCIENCE NEWS**

www.advancedsciencenews.com

**ADVANCED
MATERIALS**

www.advmat.de

[160] Z. Yan, F. Zhang, F. Liu, M. Han, D. Ou, Y. Liu, Q. Lin, X. Guo, H. Fu, Z. Xie, M. Gao, Y. Huang, J. Kim, Y. Qiu, K. Nan, J. Kim, P. Gutruf, H. Luo, A. Zhao, K. C. Hwang, Y. Huang, Y. Zhang, J. A. Rogers, *Sci. Adv.* **2016**, *2*, e1601014.

[161] A. Rafsanjani, K. Bertoldi, *Phys. Rev. Lett.* **2017**, *118*, 084301.

[162] E. Hawkes, B. An, N. M. Benbernou, H. Tanaka, S. Kim, E. D. Demaine, D. Rus, R. J. Wood, *Proc. Natl. Acad. Sci. USA* **2010**, *107*, 12441.

[163] J. H. Na, A. A. Evans, J. Bae, M. C. Chiappelli, C. D. Santangelo, R. J. Lang, T. C. Hull, R. C. Hayward, *Adv. Mater.* **2015**, *27*, 79.

[164] M. Jamal, A. M. Zarafshar, D. H. Gracias, *Nat. Commun.* **2011**, *2*, 527.

[165] S. G. A, E. A. Matsumoto, R. G. Nuzzo, L. Mahadevan, J. A. Lewis, *Nat. Mater.* **2016**, *15*, 413.

[166] Y. Iwata, E. Iwase, in *2017 IEEE 30th Int. Conf. Micro Electro Mech. Syst.*, IEEE, Piscataway, NJ, USA **2017**, pp. 231–234.

[167] S. M. Felton, M. T. Tolley, R. J. Wood, in *2014 IEEE Int. Conf. Autom. Sci. Eng.*, IEEE, Piscataway, NJ, USA **2014**, pp. 1232–1237.

[168] K. Kuribayashi, K. Tsuchiya, Z. You, D. Tomus, M. Umemoto, T. Ito, M. Sasaki, *Mater. Sci. Eng., A* **2006**, *419*, 131.

[169] J. S. Randhawa, S. S. Gurbani, M. D. Keung, D. P. Demers, M. R. Leahy-Hoppa, D. H. Gracias, *Appl. Phys. Lett.* **2010**, *96*, 191108.

[170] T. H. Ware, M. E. McConney, J. J. Wie, V. P. Tondiglia, T. J. White, *Science* **2015**, *347*, 982.

[171] Q. Ge, C. K. Dunn, H. J. Qi, M. L. Dunn, *Smart Mater. Struct.* **2014**, *23*, 094007.

[172] T.-H. Kwok, C. C. L. Wang, D. Deng, Y. Zhang, Y. Chen, *J. Mech. Des.* **2015**, *137*, 111413.

[173] D. Raviv, W. Zhao, C. McKnelly, A. Papadopoulou, A. Kadambi, B. Shi, S. Hirsch, D. Dikovsky, M. Zyracki, C. Olguin, R. Raskar, S. Tibbits, *Sci. Rep.* **2015**, *4*, 7422.

[174] G. M. Whitesides, M. Boncheva, B. Y. Ahn, E. B. Duoss, K. J. Hsia, J. A. Lewis, R. G. Nuzzo, *Proc. Natl. Acad. Sci. USA* **2002**, *99*, 4769.

[175] Y. Liu, J. K. Boyles, J. Genzer, M. D. Dickey, *Soft Matter* **2012**, *8*, 1764.

[176] T. G. Leong, B. R. Benson, E. K. Call, D. H. Gracias, *Small* **2008**, *4*, 1605.

[177] P. Tyagi, N. Bassik, T. G. Leong, C. Jeong-Hyun, B. R. Benson, D. H. Gracias, *J. Microelectromech. Syst.* **2009**, *18*, 784.

[178] W. J. Arora, A. J. Nichol, H. I. Smith, G. Barbastathis, *Appl. Phys. Lett.* **2006**, *88*, 053108.

[179] Z. Liu, H. Fang, K. W. Wang, J. Xu, *Mech. Syst. Signal Process.* **2018**, *108*, 369.